

FM4017 Project 2019

# Solar Panel Data Collection and Heat Balance



MP-13-19

Faculty of Technology, Natural sciences and Maritime Sciences  
Campus Porsgrunn

**Course:** FM4017 Project, 2019

**Title:** Solar Panel Data Collection and Heat Balance

This report forms part of the basis for assessing the student's performance in the course.

**Project group:** MP-13-19 Solar Panel      **Availability:** Open

**Group participants:** Vafa Ahmadi (222126)  
Marianne F. Heitmann (222495)  
Marthe Nergård (121810)  
Seyyedarash Zarrinkia (222121)

**Supervisor:** Kjell-Arne Solli  
Hans-Petter Halvorsen

**Summary:**

Solar energy usage in households and larger industries has become convenient in recent years. The use of solar power as electricity in Norway is a field of research in order to investigate optimum conditions in terms of location and weather conditions for the placement of solar panels. Solar panels have higher efficiency at a temperature lower than 25°C at constant sun irradiation. Thus, proper operational conditions to operate solar panels are expected in Norway. This technical report represents a study on data acquisition related to outdoor solar power measurements and modeling in order to have a prediction tool.

The work is done on three main parts. First, a study on operating devices to set up the system in order to collect operational data such as the panel surface temperature, ambient temperature, power, and the sun irradiation. Second, saving solar power data and make a cloud database. Third, simulation of the solar panel heat balance, power generation, and grid DC/AC inverter. Furthermore, develop a weather data saving application and export data to the cloud database.

Data collection outcomes in this project were detecting the correct sequence for solar power measurement, gathering solar data, investigating the possibility of automatic data collection. Finally, the automatic data saving procedure for temperature data was found. In addition, the weather data application worked properly to save data and all data were stored in a specific cloud database.

Simulation results in power generation were in agreement with the real measurements with an error of less than 3.3%. The heat balance simulation was valid as well because it showed numbers between the surface and the back of the panel. At last, a simple DC/AC inverter was simulated and explained.

*The University of South-Eastern Norway takes no responsibility for the results and conclusions in this student report.*

# Preface

The members of this group would like to thank the University of South-Eastern Norway (USN), the supervisors Kjell-Arne Solli and Hans-Petter Halvorsen, and all other staff that helped us during this project. Despite the difficulties with IIA parts that needed enough skills of software, control, and automation engineering, the group as PT and EET student could manage to complete most of the tasks during the short time of the project.

Furthermore, the group faced an unexpected 5 weeks delay receiving the devices. Therefore, started working on weather station application which was defined as an optional task. This caused limited timing for the automation of solar panel data collection.

However, it was a good experience for time management, teamwork and obtaining new skills as engineers.

Porsgrunn, 20.11.2019

Vafa Ahmadi

Marianne F. Heitmann

Marthe Nergård

Seyyedarash Zarrinkia

# Contents

Preface .....	3
Contents.....	4
Nomenclature .....	7
<b>1 Introduction .....</b>	<b>8</b>
1.1 Background of Photovoltaic Systems .....	8
1.1.1 Solar Energy .....	8
1.1.2 Photovoltaic Cells and Solar Panels .....	9
1.1.3 Solar Panels in Norway .....	9
1.1.4 Solar Panel Rafts.....	10
1.2 Bachelor Thesis Background .....	10
1.3 Project Goals.....	10
1.4 Potential Project Limitations .....	11
<b>2 Description of the Solar Panel System .....</b>	<b>12</b>
2.1 The Solar Panel .....	12
2.2 Electronic Load .....	13
2.3 Temperature Data Logger .....	14
2.4 Temperature Sensors .....	14
2.5 Spectrometer .....	15
2.6 Data Acquisition.....	17
2.7 Cloud Database / Service .....	17
<b>3 Sun Irradiation.....</b>	<b>18</b>
<b>4 PV Power Generation.....</b>	<b>20</b>
4.1 Semiconductor layer .....	20
4.2 Diodes .....	21
4.3 Theoretical Model of Solar Panel Circuit.....	21
4.4 Ideal Cell Single-diode Model .....	22
4.5 Circuits with Resistors .....	24
4.5.1 Single-diode $R_s$ Model .....	24
4.5.2 Single-diode $R_p$ Model .....	25
4.6 Shading.....	27
4.7 DC/AC inverter .....	27
<b>5 Heat Balance .....</b>	<b>28</b>
5.1 Energy Absorption by the PV Module .....	29
5.2 Heat Transfer Forms.....	33
5.2.1 Radiation .....	33
5.2.2 Conduction .....	34
5.2.3 Convection.....	35
5.2.4 Panel in Horizontal Position.....	37
5.2.5 The panel in Angled Position.....	38
<b>6 Simulation.....</b>	<b>39</b>
6.1 Simulation the Power Generation .....	39
6.1.1 Assumptions.....	39
6.1.2 Constant Parameters .....	39
6.1.3 Power Generation in Simulink .....	40
6.2 Heat balance Simulation .....	44
6.2.1 Assumptions.....	44
6.2.2 Parameters.....	45
6.2.3 Heat Balance for Closed-Circuit .....	45
6.2.4 Heat Balance for Open-Circuit.....	46
6.2.5 Shading Effects .....	47

6.3 DC/AC Inverter .....	47
6.3.1 Parameters.....	47
6.3.2 Model in Simulink.....	47
<b>7 Application for Weather Station.....</b>	<b>49</b>
7.1 Weather Station Description.....	49
7.1.1 Capricorn 2000EX Weather Station .....	49
7.1.2 The Weather MicroServer.....	50
7.2 Automatic Data Collection from the Weather Station .....	50
7.3 Developing the Application to Save Weather Station Data .....	51
7.3.1 ModBus protocol.....	51
7.3.2 Developing the application .....	52
<b>8 Practical Experiment.....</b>	<b>55</b>
8.1 Requirements .....	55
8.2 Setting Up Devices and Connections .....	55
8.3 Software Set up and Operation .....	56
8.3.1 Set Up LinkView .....	56
8.3.2 Set Up Squirrel View .....	57
8.3.3 Set Up SpectraWiz .....	58
8.4 Mounting the Panel on the Roof.....	60
<b>9 Data Collection .....</b>	<b>61</b>
9.1 Electrical Data Collection.....	61
9.2 Temperature Data Collection.....	63
9.3 Irradiance Data Collection .....	63
<b>10 Database.....</b>	<b>64</b>
10.1 Description of Database and Cloud Storage .....	64
10.2 Developing a Database in Microsoft SQL Server .....	64
10.3 Database for the Weather Station .....	65
10.4 Database for Solar Panel Measurements.....	65
10.5 Cloud Storage .....	66
<b>11 Results .....</b>	<b>67</b>
11.1 Solar Panel Data Collection .....	67
11.1.1 Electronic Load Data.....	67
11.1.2 Temperatures measured by the Data Logger.....	68
11.1.3 Data Collection with the Spectrometer and Weather Station .....	68
11.2 Weather Station .....	69
11.3 Calculations.....	70
11.4 Simulation Results .....	72
11.4.1 I-V, P-V Curves.....	72
11.4.2 Heat Balance Simulation .....	73
11.4.3 DC/AC Simulation.....	74
<b>12 Discussion .....</b>	<b>76</b>
12.1 Solar Panel outdoor measurements .....	76
12.1.1 Electric Data.....	76
12.1.2 Temperature Data.....	77
12.1.3 Irradiance Data .....	77
12.1.4 Weather station .....	77
12.2 Simulation.....	78
12.2.1 Power Generation Simulation .....	78
12.2.2 Heat Simulation .....	78
12.2.3 DC/AC inverter.....	79
<b>13 Conclusion.....</b>	<b>80</b>
<b>14 Further Work.....</b>	<b>81</b>
<b>References.....</b>	<b>82</b>

**Appendices .....85**

# Nomenclature

HSLV	High Signal Low Voltage
LSHV	Low Signal High Voltage
MPP	Maximum PowerPoint
NOCT	Nominal Operating Cell Temperature
OC	Open Circuit
PV	Photo Voltaic
SC	Short Circuit
SQL	Structured Query Language
STC	Standard Test Conditions
$\alpha$	The angle of the solar panel
$\delta$	Absorptivity of the surface
$\theta$	Angle of sun array with normal direct irradiation
$\rho$	Reflectivity
$\tau$	Transmissivity
$\chi$	Thermal diffusivity

# 1 Introduction

This technical report is divided into theory, practical work, simulation, and data acquisition.

Chapter 1 is an introduction to solar energy and the background of the project.

Chapter 2 is about the solar panel system description.

Chapter 3 contains a brief theory of the sun irradiation.

Chapter 4 gives an overview of power generation and DC/AC inverter.

Chapter 5 gives an overview of heat balance equations.

Chapter 6 is about the simulation of power generation, heat balance, and DC/AC inverter.

Chapter 7 is about developing a weather data saving application.

Chapter 8 describes the practical work with the solar panel and setting up its additional devices.

Chapter 9 is about the data collection procedure with software and the possibility of automatizing data collection.

Chapter 10 describes the data storage procedure.

Chapter 11 contains the results.

Chapter 12 contains the discussion of the results.

Chapter 13 contains the conclusion.

Chapter 14 is about the further work.

The following chapter contains the background of photovoltaic systems, the background of this project, the project goal and the limitations of the project.

## 1.1 Background of Photovoltaic Systems

This section is about a brief summary of solar energy, photovoltaic (PV) cells, use of solar panels in Norway, solar panels on rafts and what was done in the bachelor thesis at the University of South-eastern Norway during spring 2019.

### 1.1.1 Solar Energy

Solar energy consists of light and heat radiation from the sun. The sun is one of the primary energy sources for life on earth and the total solar energy that reaches the earth in one year is 15 000 times higher than the required energy consumption of the whole world. The radiation that reaches the earth is significantly low compared to the radiation and light on the sun itself. The atmosphere and clouds absorb 54 % of the radiation, which gives 50 % visible light, 45% infrared radiation and modest amounts of UV-radiation and electromagnetic radiation. Figure 1.1 shows how the photovoltaic power potential varies at different locations on earth. Though the solar energy reaching the earth has immense potential, the cost of conversion to electricity and thermal energy is limited. The process has low efficiency and high costs. [1] [2]



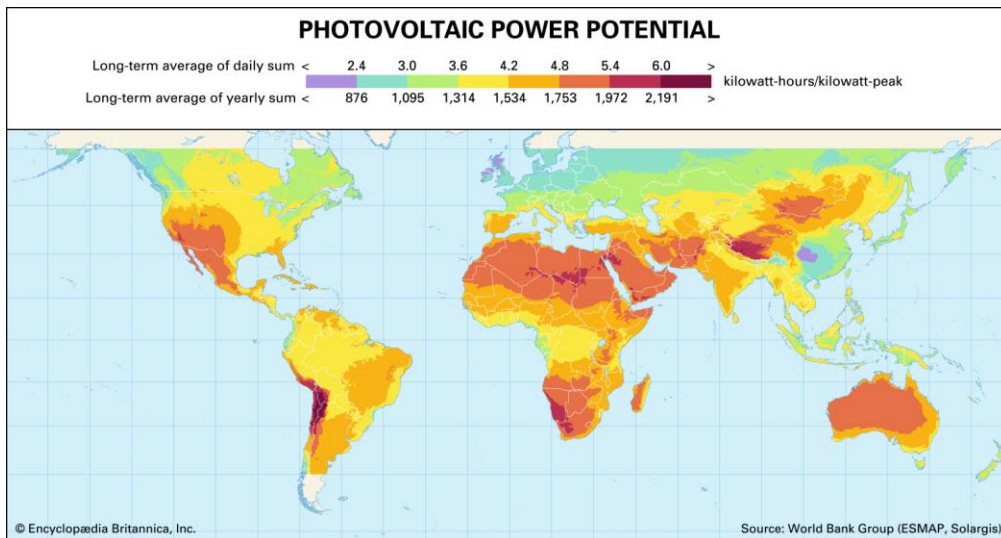


Figure 1.1: Illustration of photovoltaic power potential[3].

### 1.1.2 Photovoltaic Cells and Solar Panels

Photovoltaic cells convert the energy of sunlight into electric energy with the photovoltaic effect. The photovoltaic effect produces an electrical voltage between two materials when struck by light or radiation. [4] [1]

Photovoltaic modules do not provide a constant electric voltage or current intensity. This depends on the number of instruments connected, solar irradiation at every moment and temperature of the solar cell. Photovoltaic (PV) modules convert sunlight directly to electric energy without any engines or rotating equipment. The photovoltaic cells are made up of two or more layers of semiconductors, the whole semiconductor layer is also called wafer. The most common are silicon (Si), compounds of cadmium sulfide (CdS), cuprous sulfide (Cu<sub>2</sub>S), and gallium arsenide (GaAs). When the sunlight hits the PV module, electrical charges are produced. There is no emission of greenhouse gases in the energy production. [5]

Photovoltaic solar panels use photovoltaic cells to convert sunlight and convert directly to electricity. The efficiency of a solar panel varies from 16-20% depending on weather conditions, shade, pollution of the panel surface and temperature of the panel. With increasing the temperature of the solar panel, the efficiency drops significantly. The solar cells have a lifespan of 20 to 40 years. [6]

### 1.1.3 Solar Panels in Norway

In theory, the ideal placement of a solar panel is located near the equator. This area has high sun radiation, few rainy days and the smaller amount of clouds. These conditions also cause a high operating temperature for the solar panels, which decreases efficiency. In Norway, the weather varies, but the operating temperature is ideal. SINTEF's experiment concludes that the use of solar energy in Norway is effective in spite of harsher weather conditions. During the winter, the reflection of the snow and the low temperature creates ideal conditions for a solar panel. Even rain and ice on the panels did not inhibit efficiency. The Norwegian climate still has some challenges with limited light during the winter and the amount of snow shading the panel. [7]

### 1.1.4 Solar Panel Rafts

Floating solar panel power plants is a new way to utilize solar energy in alternative locations. The market for floating solar power is increasing and is expected to reach 10 GW by 2030. The advantage of solar panels on rafts is the cooling effect of the water and to be able to utilize hydropower reservoirs for solar energy as well. The challenging parts are the unknown effects of the motion in the water, wind, aquatic environment around the rafts and birdlife surrounding the area.

A solar panel raft consists of floating rings made of plastic, a membrane, anchoring system to the bottom of the water and the solar panels on top. The rafts require small amounts of material per kilowatt electricity produced which is beneficial economically and environmentally.

Statkraft will complete its first floating solar power plant in 2020 in its hydropower plant in Albania. [8]

Ocean Sun AS is a Norwegian company specializing in PV modules on floating rafts. The company started its research and experimentation in 2016 and have tested systems on the Norwegian west coast. Ocean sun offers several horizontal modules with a recommended angle of 45 degrees. [9] [10]

Multiconsult is also researching the possibility of using floating solar panels in combination with hydroelectric power. The project is led by Stanislas Merlet as a Ph.D. study focusing on how hydropower and solar power can be combined and optimize electricity generation. [11] [12]

## 1.2 Bachelor Thesis Background

The background of this project is a bachelor thesis written by engineer students at USN spring 2019 in partnership with Suncells Sea Norway AS. The topic of the thesis was design, construction, and testing of a test rig for alternative placements of solar panels. The solar panel was tested outside on the roof of USN and inside with a special built light rig. The thesis concluded that the efficiency of the solar panel would increase by 34,5% annually by turning the solar panel in an angle with the sun. By using water as a surface, the temperature of the solar panel would preserve a lower temperature and high efficiency. [13]

## 1.3 Project Goals

The main goals of this project are data acquisition and instrumentation for heat balance and the performance of PV systems. This goal is set to:

- Collect data from the solar panel based on outdoor measurements as well as data collection from the weather station.
- Compare the irradiation data from the spectrometer with standard ASTM reference spectra.
- Develop a heat balance model that can predict the silicon layer (wafer) temperature based on air temperature and irradiation data. Use the heat balance simulation model for the prediction of solar panel layer temperatures based on air temperature, surface characterization and irradiation data.
- Simulate the heat balance of the solar panel with a simulation tool for power estimation based on the local climate.
- Develop a weather data saving application and store data.

- Develop three separate automatic procedures for panel temperature measurements, solar panel power generation, spectral data and demonstrate the data collection.
- As an optional task, place a solar panel on a raft to compare the power generation with land placement, if possible.
- Include DC/AC inverter variables and properties into a simulation model for power generation, if possible.

## 1.4 Potential Project Limitations

The limitations during the work in this project might be:

- The duration of this group project is 2.5 months.
- If no fixed place is provided in the time of the project, no valuable data can be obtained in order to have historical data collection. Because the solar panel should have an appropriate placement with open exposure to sun irradiation. In this condition, the outdoor measurement will be carried out only for testing the panel and simulation.
- On rainy and snowy days, the outdoor measurements are not possible as long as no fixed place is provided.
- Shading effect observation needs appropriate conditions. It can be discovered if the placement is set.
- The automatizing data collection part needs a strong knowledge in IT, software and control engineering. Since there is no IIA student in the group and the short duration of the project, these tasks may end with the possibility assessment of automatizing data collection.
- No external partner might be involved in this project.
- Cost approval from USN in order to provide potential software for programming may take long.
- Using older versions of devices and lacking some connection features may make automatic data collection not possible.
- If no external partner is available, the placement on rafts can not be done.
- To simulate DC/AC variables, an inverter should be provided to connect the solar power to the electricity grid. If it is not provided no real data will be available to be used in the simulation.

## 2 Description of the Solar Panel System

The following chapter contains a description of the solar panel system with all the equipment used in this project.

Figure 2.1 illustrates a sketch of the PV system used in this project. The data logger is connected to the computer with a USB cable and to the solar panel with the temperature sensors. The load module (electronic load) is also connected to the computer with a USB cable and the solar panel with IBC Flexisun 1x6mm<sup>2</sup> cables. The spectrometer is connected to the computer with a USB cable. Detail description of the equipment follows in this chapter.

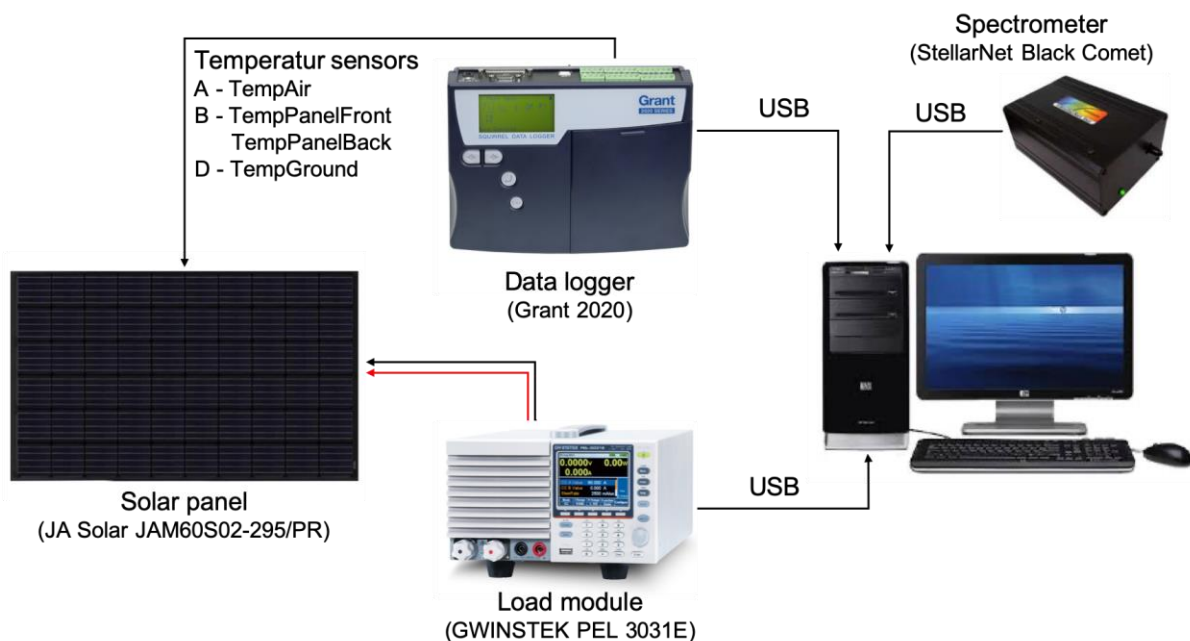


Figure 2.1: A sketch of the PV system. Sketch made with figures from [14-18]

### 2.1 The Solar Panel

The PV system consists of a monocrystalline solar panel from JA Solar called JAM60S02-295/PR. Figure 2.1 shows the solar panel used in this project.

The photovoltaic module (solar panel) consists of 60 mono cells and has a nominal power of 295 W. Table 2.1 contains the data of the panel.

Table 2.1: Specifications and operating conditions of the Solar panel. [19]

Specifications		Operating Conditions	
Cell	Mono 156.75× 156.75 mm	Maximum System Voltage	1000V DC (IEC)
Weight (kg)	18.2 kg ± 3%	Operating Temperature	-40°C ~ +85 °C
Dimensions (L×W×H) (mm)	1650 × 991 × 35 mm	Maximum Series Fuse	20 A
Cable Cross Section Size	4 mm <sup>2</sup>	Maximum Static Load (Front)	5400 Pa
No. of cells	60 (6×10)	Maximum Static Load (Back)	2400 Pa
Junction Box	IP67, 3 diodes	NOCT	45±2 °C
Connector	MC4 compatible	Application Class	Class A
Packaging Configuration	30 per pallet		

NOCT means normal operating cell temperature that is a standard term to solar cells operating conditions. When the solar panel is at standard testing condition (STC), i.e. it is tilted with the angle of 45° and operating open circuit cells at 800 W/m<sup>2</sup> of irradiation, environment temperature of 20°C and 1 m/s wind speed with the open backside of the panel, it reaches to NOCT Temperature. [20]

## 2.2 Electronic Load

GWINSTEK PEL 3031E is a single channel electronic load with a maximum power of 300 W, 60 A current and voltage range from 1 to 150 V. It is used to analyze the voltage, current, and power and dissipate the generated power from the solar panel in a safe way. Seven modes are defined in programming this load module for operation, constant current CC, constant voltage CV, Constant resistance CR, Constant power CP. [21]

These four modes are for basic operations and CC+CV, CR+CV, CP+CV are for combined operations. Sinking current is done from 60 mill Amps (mA) to have operational measurements of a power generation via the solar panel. [21]

Based on the solar panel operating conditions, the device will sink constant current in CC mode in accordance with the set current value. In CV mode, the load module controls the source voltage with sinking corresponding current to that voltage according to a set value of voltage. In CR mode, the resistance will be set to a constant value and the device will sink the corresponding current and voltage which have a proportionally linear relation with each other. In CP mode, a constant power will be set, and the device will initiate the power according to the voltage and current which give that power. [21]

To be able to switch between two operating modes, the dynamic mode should be set. The sequence function is to make more than two operating modes in to switch in sequence. The sequencing types normal sequence and fast sequence. The normal sequence is a flexible way to have measurements with the different four operating modes and adjusting time from 1

millisecond to 59 seconds, 59 minutes or 999 hours. The load module can be seen Figure 2.2. [21]



Figure 2.2: The load module GWINSTEK PEL 3031E. [22]

### 2.3 Temperature Data Logger

To measure the temperature of the air around the solar panel, the front and back temperature of the solar panel and the temperature at the ground, the data logger Squirrel (SQ) 2020 series from Grant Instruments is used. This is user-defined, and the user can connect the sensors needed to the any of the blocks. It has 8-16 universal inputs. To measure the temperature four sensors are used, in three blocks. A is the air above the solar panel, B is for the front and back panel temperature (two sensors in one input) and D is for the ground temperature. Figure 2.3 shows the Grant SQ2020 data logger both the front and the top with the inputs visible. [23]



Figure 2.3: The Grant SQ2020 data logger in front and top with the blocks visible. [15]

### 2.4 Temperature Sensors

PT1000 platinum resistance thermometers are used to measure the temperatures around the solar panel and the surface of the solar panel. This thermometer gives accuracy over a wide range of temperatures, from  $-200^{\circ}\text{C}$  to  $+850^{\circ}\text{C}$ . It is available with numerous packaging options and different accuracy specifications to fit most applications, and unlike thermocouples, a special cable to connect the sensor is not needed. The thermometer works by measuring the resistance of the platinum element. The PT1000 sensor has a resistance of 1000

ohms at 0°C. Over a small temperature range, the relationships between resistance and temperature are nearly linear. To get the precise temperature, it is needed to linearize the resistance. This linearization is obtained by equation (2.1). [24]

$$R_t = R_0(1 + A t + B t^2 + C(t - 100) t^3) \quad (2.1)$$

Where:

$R_t$  is the resistance at temperature  $t$ ,

$R_0$  is the resistance at 0°C,

$A = 3.9083E-3$ ,

$B = -5.775 E-7$ ,

$C = -4.183 E-12$  (below 0°C), or  $C = 0$  (above 0°C).

For this sensor, a 0.384-ohm change in the resistance will occur at 1°C temperature change. So even a small measurement error can cause a big error in the temperature measurement. The sensors have four wires, two of the sensors carry the sense current, while the other two sensors measure the voltage across the sensor element. A three-wire sensor is also available, but it operates under the assumption that the resistance of each of the wires is the same. [24]

## 2.5 Spectrometer

A spectrometer is an optical instrument that measures the intensity of light as a function of wavelength and frequency. The spectrometer receives light and breaks it down into spectral components. These components are then converted into digital signals as a function of wavelength and displayed on a computer. [25]

The spectrometer used in this project is a Stellar Net spectrometer of the Black-comet series as shown in Figure 2.4. Model CXR-SR delivers high-performance spectroscopy in the UV-VIS-NIR wavelength from 400-1100 nm. This range of wavelength corresponds to the visible light which is absorbed by the solar panel. Visible light has a range of 350-1140 nm. The spectrometer has several features such as improved spectral shapes, stray light reduction, enhanced sensitivity, uniform resolution, and thermal stability. It can be connected to a computer using a USB-port. [26]



Figure 2.4: Illustration Stellar Net Black Comet CXR-SR. [26]

The spectrometer is connected to a sensor when making irradiance measurements. The sensor has a  $180^\circ$  range of light measurement and measures in cosines waves. The setup of the spectrometer with the sensor is shown in Figure 2.5.



Figure 2.5 The set up with spectrometer and sensor.



## 2.6 Data Acquisition

Data acquisition (DAQ) is the process of measuring an electrical or physical phenomenon such as voltage, current, temperature, pressure, or sound with a computer. A DAQ system consists of sensors, DAQ measurement hardware, and a computer with programmable software. Compared to traditional measurement systems, PC-based DAQ systems exploit the processing power, productivity, display, and connectivity capabilities of industry-standard computers providing a more powerful, flexible, and cost-effective measurement solution. [27]

A computer with programmable software controls the operation of the DAQ device and is used for processing, visualizing, and storing measurement data. Different types of computers are used in different types of applications. A desktop may be used in a lab for its processing power, a laptop may be used in the field for its portability, or an industrial computer may be used in a manufacturing plant for its ruggedness. [28]

## 2.7 Cloud Database / Service

A database is a collection of information or data which can be easily managed, organized or updated. Databases are in many different forms such as relational databases, graph databases, cloud database or many different other forms. In this project, the main focus is about the relational databases in which information is sorted out with respect to their date and the time they are saved. [28]

Another example that is of this project interest is a cloud database. A cloud database is a set of information stored in a virtualized environment where it can be either as public database or private or as a hybrid one. A cloud database resides on servers and storage furnished by a cloud or database as a service (DBaaS) provider and it is accessed solely through the internet. To a software application, for example, a SQL database residing on-premises or in the cloud should appear identical. [28]

### 3 Sun Irradiation

The radiation from the sun is modified by several obstacles before reaching the solar panel. These modifications are absorption and scattering through the atmosphere. As mentioned in chapter 1.1.1, 54% of the radiation is absorbed by the atmosphere and clouds. The scattering redirects the radiation from the sun and this affects the amount of light reaching the solar panel. Rayleigh scattering is caused by small gas molecules and causes approximately uniform scattering in every direction. Mie scattering is caused by dust and soot particles of larger size and performs scattering in the original direction of the sun rays. The absorption and scattering of solar radiation cause diffusive radiation reaching the solar panel. [29]

As can be seen in Figure 3.1, solar arrays irradiate to earth with an angle according to daily hours. In order to obtain direct irradiation, correction with the irradiation angle is required.

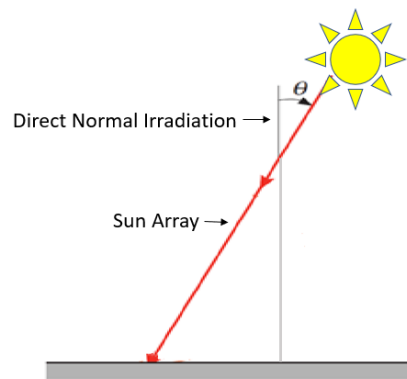


Figure 3.1: The angle of solar arrays with the ground<sup>1</sup>. [29]

$G_0$  is defined as the direct irradiation to the earth from the sun considering the angle  $\theta$ . It is obtained by equation (3.1). [29]

$$G_0 = G_s \cos(\theta) \quad (3.1)$$

$G_n$  is the irradiation that comes to the PV panel from the sun. The amount of solar irradiation and the angle of irradiation is found from weather station parameters. If the PV panel is mounted by angle  $\alpha$ , another correction due to this angle should be considered as given in equation (3.2).<sup>2</sup> [29]

$$G_n = G_s \cos(\theta) \cos(\alpha) \quad (3.2)$$

<sup>1</sup> The figure in the reference is edited in this chapter.

<sup>2</sup> This equation is obtained based on the information in the book.

It is found from Porsgrunn average climate that the average solar energy per square meter in November changes as shown in Figure 3.2.

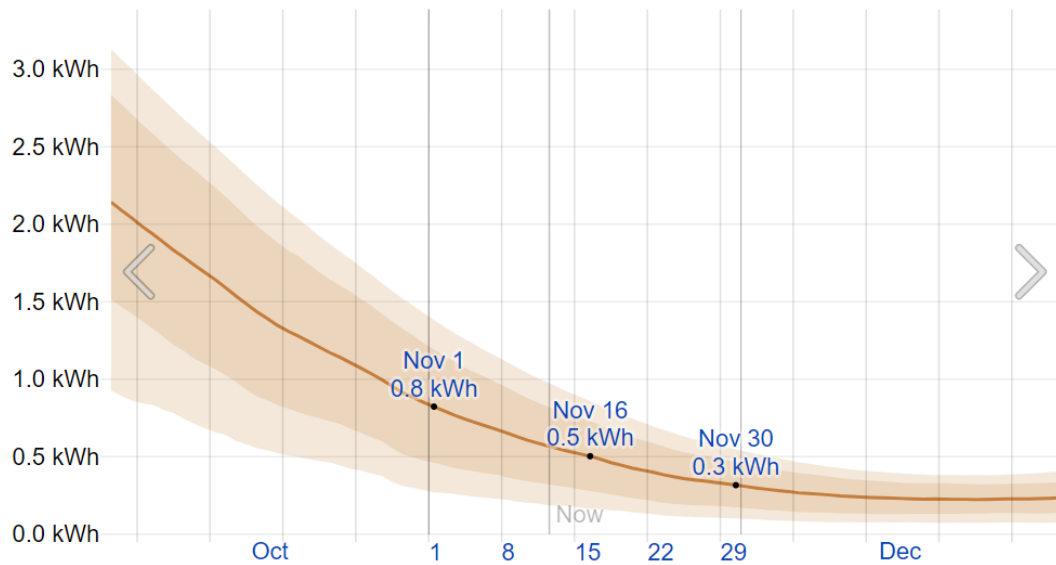


Figure 3.2: Average solar incident per square meter in November in Porsgrunn. [30]

This means in the short days of November the sun irradiation during the day is between 0.8 KW per hour and 0.3 KW per hour. [30]

## 4 PV Power Generation

This chapter gives an overview of the theory of semiconductors, their functionality in solar cells, diodes, their use in solar panels. In addition, the theory of solar panel circuits is explained to be used in simulation the power generation.

### 4.1 Semiconductor layer

The sun's energy emission is in the form of waves. As described in the introduction chapter, the wavelengths are classified in three ranges, ultraviolet (short wavelength), visible, (rainbow of the visible spectrum), infrared. (long wavelength). During the sunshine, these waves come towards the earth and hit the surface of the solar cells. These photovoltaic cells generate electricity from the sun.

The structure of the active part of the cell is shown in Figure 4.1. This part is a wafer made of silicon (Si) which is a semiconductor material. This element becomes conductive and generates electricity when it is exposed to sun or artificial light. The semiconductor part of the solar cell is made of three thin layers. The top layer consists of silicon and few negatively charged elements as phosphorus (P), this layer is called negative type (n-type) because it transports free electrons. The layer in the bottom of the wafer is made of silicon and an element such as boron (B).

Phosphorous has more electrons than silicon while boron has fewer electrons than that. Lack of electrons makes the bottom layer as an effective positive charge layer, so it is called p-type or positive layer. The positive layer can be assumed as a positive dope that has holes in it. [31]

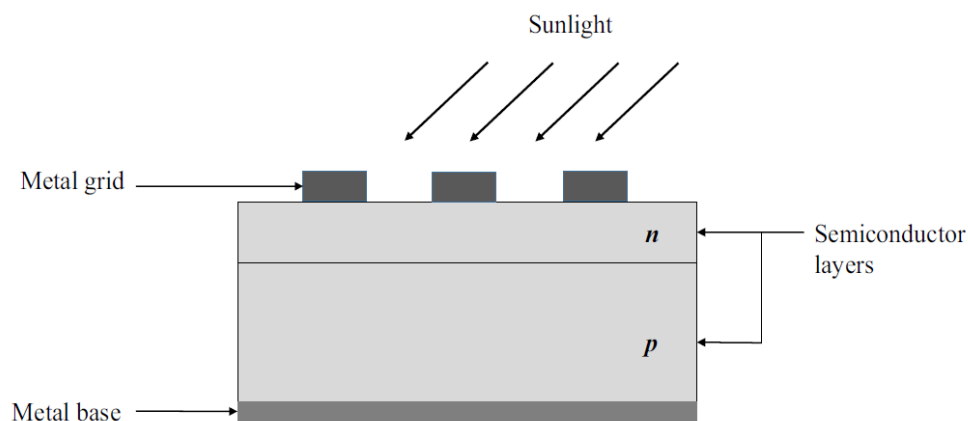


Figure 4.1: A photovoltaic cell structure with n-p junction [32].

The thin fin metal grids are commonly made of silver on the top. At the bottom, the metal base is typically an aluminum plate. Wavelength of 350- 1140 nm including the visible spectrum can absorb the solar cell and rich the middle layer of the silicon wafer. Ultraviolet wavelengths are stopped at the wafer surface.

Infrared wavelengths will pass the panel and go out of the aluminum plate. The sun wave strikes the silicon making it lose an electron. When the silicon atom becomes positive, called hole, it moves to the positive layer which has many positive dopes. Free electrons move to the top layer. Such activity in the n-p layer continues during the day until sunlight is available. The

metals on the top and at the bottom work as electrodes. Connecting the electrodes to DC wires, makes negative and positive charge flow through them which is electric current and power are generated. [33] [32] [31]

## 4.2 Diodes

Diodes are electrical devices that allow the current pass through them or block the current. In other words, diodes act such as a valve for electric current. When electric potential is applied across the diode, if the diode allows the current to pass, it is called forward-biased diode. If the diode stops the current, it is called a reverse-biased diode. A very small amount of current can pass through the reverse-biased diode that is called leakage current. If the reverse voltage which causes reverse current is high, the diode will be damaged. This condition is called diode breakdown. [34]

Semiconductors are a type of diode. The saturation current in semiconductor diodes is the maximum current which can be obtained from a semiconductor in certain operating conditions. Reverse saturation current is the current caused by diffusing the positive charge carriers to the neutral region in the p-n junction.[34]

## 4.3 Theoretical Model of Solar Panel Circuit

In order to simulate the power generation, the electrical model of the solar panel is required. Solar panel efficiency  $\eta$  can be defined as equation (4.1).

$$\eta = \frac{P_{mpp}}{P_{in}} \quad (4.1)$$

Where  $P_{mpp}$  (W) is the maximum electricity generated in the solar panel and  $P_{in}$  (W) is the total power of light incident to the PV panel.  $P_{in}$  can be calculated from equation (4.2).

$$P_{in} = G_n - \delta G_n \quad (4.2)$$

Where:

$G_n$  is the sun irradiation to the solar panel,

$\delta$  is the absorptivity of the solar panel layers,

The term  $\delta G_n$  corresponds to the absorbed energy which converts to heat in the solar panel and causes the increase in layer temperature.

PV cells are one type of semiconductor and are assumed as diodes. In order to model the power generation, specification of the system is required. PV cell circuits can be in parallel or series configuration with one-diode, two-diode or three-diode model. It is found that JAM60S02-295/PR is based on a single-diode model according to its datasheet. The solar cell junction is an n-p junction in the panel. Figure 4.2 shows a typical scheme of PV cell operation. [35]

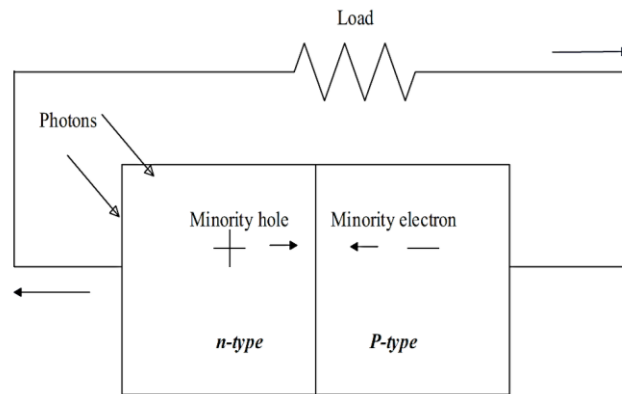


Figure 4.2: A simple scheme of PV cell operation [32].

Diodes connected in series show the equivalent current when the voltage is generated in the solar panel. The commercial solar panels have a junction box. In this box, commercial diodes are used to pass the total current of the solar panel. Commercial diodes have different capacities and they are selected based on the solar panel's power generation capacity. [36]

In the following section, the single-diode model, the relevant model to this solar panel, will be described. [32]

#### 4.4 Ideal Cell Single-diode Model

An ideal single-diode model circuit is shown in Figure 4.3.

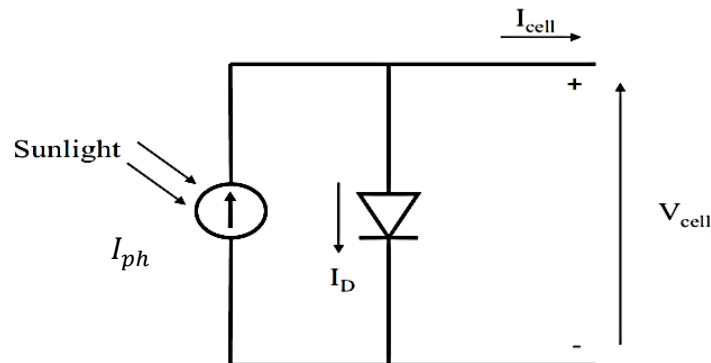


Figure 4.3: The circuit of an ideal single-diode model [32].

The net current  $I_{cell}$  from one PV cell is given in equation (4.3).

$$I_{cell} = I_{ph} - I_D \quad (4.3)$$

$I_{ph}$  is the photovoltaic current which is defined as the current generated by light and expressed in equation (4.4).

$$I_{ph} = \frac{I_{sc} + (k_i(T_{cell} - 298)) G_n}{1000} \quad (4.4)$$

Where:

$I_{sc}$  is the short circuit current<sup>3</sup> (A),

$k_i$  is the current coefficient of the solar panel,

$T_{cell}$  is the temperature of the PV cell (K),

$G_n$  is the sun irradiation intensity (W/m<sup>2</sup>). [37]

Thermal voltage, the voltage generated by electron movement during the photovoltaic mechanism, of the semiconductor is given in equation (4.5). [32]

$$V_T = \frac{nKT_{cell}N_s}{q} \quad (4.5)$$

Where:

$N_s$  is the number of solar cells in the solar panel which are connected in series.

In equation (4.3),  $I_D$  is the current passing the diode which is assumed to be parallel to the PV cell, according to the electric potential (generated voltage).  $I_D$  is calculated by equation (4.6) (Shockley expression).

$$I_D = I_0 \left[ \exp\left(\frac{qV_D}{nKT_{cell}N_s}\right) - 1 \right] \quad (4.6)$$

Where:

$I_0$  is the saturation current of the PV cell (A),

$q$  is the electron charge number that is equal to  $1.602 \times 10^{-19}$  (c).

$n$  is the ideality factor of the diode.  $n=1$  shows an ideal diode while  $n > 1$  shows a nonideal diode. The diode ideality factor differs from 1 to 2,

$V_D$  is the voltage across the diode and is found in the diode specification sheet (V),

$K$  is the Boltzmann constant equal to  $1.38065 \times 10^{-23}$  (J/K),

$T_{cell}$  is the diode temperature (K),

The saturation current,  $I_0$ , is defined by equation (4.7).

---

<sup>3</sup> Connecting two nodes in circuit in a way to obtain the same voltage in both nodes in order to have the highest current. Meaning no resistance is between the two nodes, so no voltage drop happens.

$$I_0 = I_{rs} \left( \frac{T_{cell}}{T_n} \right)^3 \exp \left[ \frac{\left( qE_g \left( \frac{1}{T_n} - \frac{1}{T} \right) \right)}{(nK)} \right] \quad (4.7)$$

Where new terms are:

$I_{rs}$  is the reverse saturation current (A),

$T_n$  is the reference temperature, 25 + 273 (K),

$E_g$  is the bandgap energy (eV) which is provided by the manufacturer, and can be found in the datasheet of solar panels. [37]

The reverse saturation current can be expressed by equation (4.8).

$$I_{rs} = \frac{I_{sc}}{\left[ \exp \left( \frac{qV_{oc}}{(nN_sKT)} \right) - 1 \right]} \quad (4.8)$$

Where the description of the new terms is:

$I_{sc}$  is the short circuit current (A).

$V_{oc}$  is the open-circuit voltage (V); corresponding to the electric potential of the circuit when its terminals are not connected to any load. It is the maximum voltage which gives the maximum power. [37]

## 4.5 Circuits with Resistors

The ideal cell model lacks some considerations to get a representative amount of maximum power obtained by a PV cell or a PV panel. Therefore, it has enough accuracy to have the basic PV cell calculations, but not enough to be used to simulate actual operating conditions.

The limitations in PV cell which affect the calculations of experimental measurements are the current loss due to series, shunt resistance and the non-ohmic recombination of the solar cell at its space-charge region (corresponding to reverse saturation current). Another factor is if the diode is not an ideal one ( $n \neq 1$ ). That is why single-diode  $R_s$  model and single-diode  $R_p$  model is defined to modify the ideal model. [32]

### 4.5.1 Single-diode $R_s$ Model

Semiconductors which the generated current goes through them are not doped completely, so they are resistive to current. Other reasons lead to total current loss due to resistivity are the resistance in the metal grid, connectors and the wires collecting the generated current. Thus, to show these resistant losses,  $R_s$  is a lumped resistor which is placed in series in the ideal model circuit as can be seen in Figure 4.4, and is called single-diode  $R_s$  model.



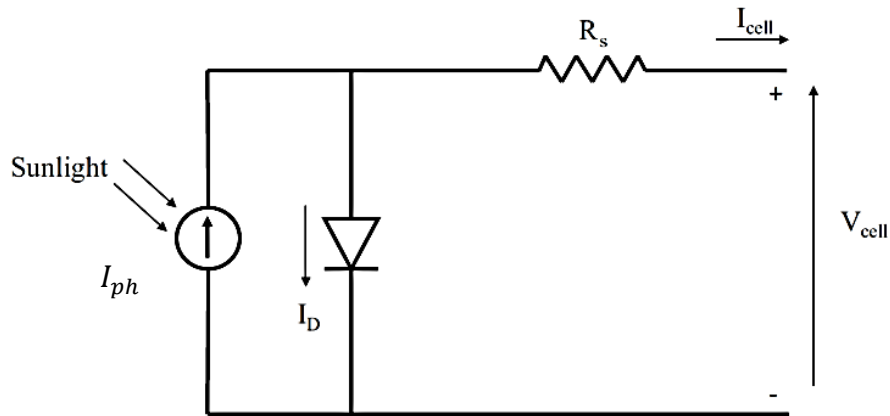


Figure 4.4: The circuit of single-diode  $R_s$  model. [32]

Equation (4.9) is an expression of the model when  $R_s$  is added. The second term on the righthand side is the diode current.

$$I_{cell} = I_{ph} - I_0 \left[ \exp\left(\frac{(V_{cell} + I_{cell}R_s)q}{nKT N_s}\right) - 1 \right] \quad (4.9)$$

Where  $R_s$  is the series resistance ( $\Omega$ ).

#### 4.5.2 Single-diode $R_p$ Model

The single-diode  $R_s$  does not consider the effect of shunt resistance, so the analytical data may not fit the practical data which give P-V and I-V curves. The circuit is shown in Figure 4.5. Shunt resistive losses mainly occur at the border of the PV cell, and in the n-type of the n-p junction. These resistances are represented by a shunt resistor placed in parallel with the diode and is indicated as  $R_{sh}$  or  $R_p$  (parallel resistors). For single diode model simulations, this model seems to be the correct model that fits practical data and structure of JAM60S02-295/PR solar panel.

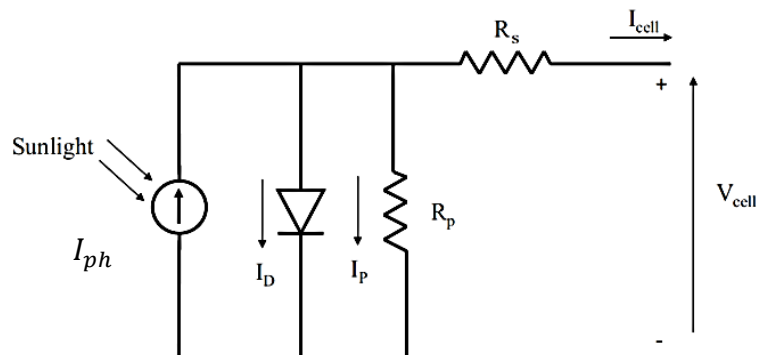


Figure 4.5: The circuit of single-diode  $R_p$  model. [32]

The current passing the parallel resistor (the shunt resistor) is calculated by equation (4.10). Then,  $I_{cell}$  with series and shunt resistance current loss is obtained by equation (4.11).

$$I_p = \frac{V_{cell} + I_{cell}R_s}{R_p} \quad (4.10)$$

$$I_{cell,s,p} = I_{ph} - I_D - I_p = I_{ph} - I_0 \left[ \exp\left(\frac{V_{cell} + I_{cell}R_s}{V_T}\right) - 1 \right] - \frac{(V_{cell} + I_{cell}R_s)}{R_p} \quad (4.11)$$

Where  $R_p$  is the parallel or shunt resistance ( $\Omega$ ) which can be found from the commercial diode datasheets.

The fill factor term is a parameter to define the quality of the solar cell. It is shown in Figure 4.6 and defined as the proportion of the current and voltage corresponding to the maximum power point ( $V_{MPP}, I_{MPP}$ ) to the multiplication of short-circuit current ( $I_{SC}$ ) and open-circuit voltage ( $V_{OC}$ ).

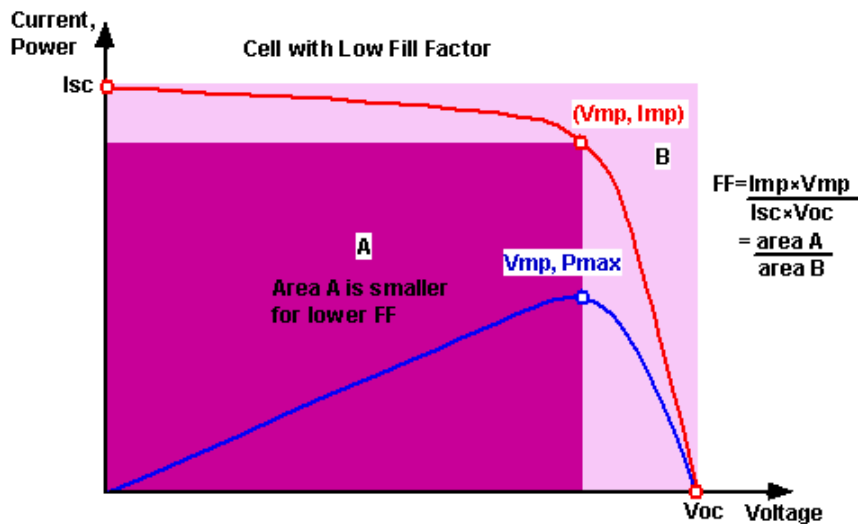


Figure 4.6: Illustration of the fill factor of a solar cell. [38]

Equation (4.12) shows the fill factor

$$FF = \frac{V_{MPP} I_{MPP}}{V_{OC} I_{SC}} = \frac{P_M}{V_{OC} I_{SC}} = \frac{\eta A_c G_n}{V_{oc} I_{sc}} \quad (4.12)$$

Where  $P_M$  is the maximum power produced in the solar cell. The values of the cells in series, Shunt resistance ( $R_{sh}$ ) and diode loss, has a direct effect on the fill factor. If the shunt resistance is increased and the lumped series resistance is decreased, the efficiency increases leading to a higher fill factor. This means the maximum practical power becomes closer to the theoretical value. The normal FF for a silicon PV cell has been found to be 80%. [38]

## 4.6 Shading

Shading the solar panel with different objects and materials works as an insulator for sun irradiation. It means that if the panel is covered by snow, heavy dust or other kinds of dirt, it affects the efficiency of power generation. The cover does not allow the sun arrays to come into the solar panel. If the thickness of the cover is high, it makes the power generation reach zero. Therefore, keeping the panel clean, and melt the snow on the panel helps with generating power closer to the maximum. The snow should be removed by heating the panel or by hot water. Wiping the panel with solid wipers might damage the glass layer as it affects the reflectivity and absorptivity of the solar panel surface. [39]

## 4.7 DC/AC inverter

Solar panels are single-phase voltage sources that produce DC voltage which is a direct constant (DC) source of power. The electricity grid is a complex grid with an alternating source of power called AC. The solar panel needs an inverter to invert the DC source of power to AC. The solar power inverter converts the DC current into 240 volts- 50 Hertz (Hz) AC electricity, which is the same as the utility grid capacity. [40]

When the DC power is converted to AC, it can be used directly to turn on electrical devices. The extra AC power goes to the utility grid. In order to have control and measurement of the amount of power which is fed to the grid, a metering device is placed at the current path. These meters are controlled by electricity companies.

Solar inverters also called grid-tied inverters, are three types. Micro, string and central inverters. A micro DC/AC inverter is used for only one solar panel, which can be placed on the back or very close to the panel. As they use less power, a safer operation is provided, but it makes the system more expensive if there are many panels.

String inverters are the commonly used inverters for households and commercial solar power systems. Many arrays can be connected to one string converter which is placed by distance from the area. Central inverters are very large string inverters used for industrial purposes, solar power plants and large buildings. Choosing inverters is due to the number of solar panels that compound solar arrays and the purpose of the system. Monitoring devices might be installed in the device or can be provided separately. [41]

A simple single-phase inverter with 50 Hz frequency, converts DC very fast to two different directions (up/down or on/off) which correspond to AC sine wave simulation.

In terms of measurements, solar inverters are a true sine wave or modified sine wave. Modified sine wave inverters are cheaper to use for simple household tools. The efficiency of these devices is about 70 % meaning that 30% of power is lost during converting to AC, so they are not recommended when the purpose is high power generation.

Sine wave inverters also known as digital inverters are much better to use for complex electric devices and more power generation. The sine wave inverter is better to be used to connect the solar panel to the utility grid. Up to 98% of DC power is converted to AC electricity by true sine wave inverters which is significantly less than modified sinewave inverters. True sine wave inverters are expensive, but less power waste makes them better to use. [42]

## 5 Heat Balance

This chapter is about the heat balance of the solar panel. The governing equations of heat balance are necessary to have a mathematical model of the system to get the idea for heat balance simulation.

In order to describe the energy balance for the solar panel, it is required to find the equations from heat transfer reference books and articles. Then make it specific for the solar panel. In order to obtain accurate heat calculation, the angle of the solar panel and different bases should be considered.

Energy balance for the system starts with equation (5.1) [29]

$$\dot{E}_{in} - \dot{E}_{out} + \dot{E}_{gen} = \dot{E}_{acc} \quad (5.1)$$

Where:

$\dot{E}_{in}$  is the internal energy to the system by time (W),

$\dot{E}_{out}$  is the energy out going out of the system by time (W),

$\dot{E}_{gen}$  is the energy generated in the system by time (W),

$\dot{E}_{acc}$  is the accumulation of energy in the system by time (W).

The internal energy is irradiation of sun to the panel which is the main source of power and heat generation. This irradiation is converted to heat and electrical power according to the mechanism of the solar panel.

A part of energy goes out of the system as heat loss. Heat transfer forms in this model are convection, conduction, and radiation. Convective heat transfer occurs when the temperature of the front and back surface of the panel becomes higher than the surrounding air. Forced convection due to windy weather conditions and natural convection due to temperature gradients between the surrounding flow and the panel surface is considered in the equation.

Conduction occurs between different layers of the solar panel because of different thermal conductivities of the materials.

Radiation occurs in two ways. Radiation from the panel to the surrounding and radiation of the ground to the back of the panel and vice versa. This means that the radiation of two planes should be considered for the back surface of the panel. [33]

Figure 5.1 shows the principle of energy forms and energy conversion through the solar panel.

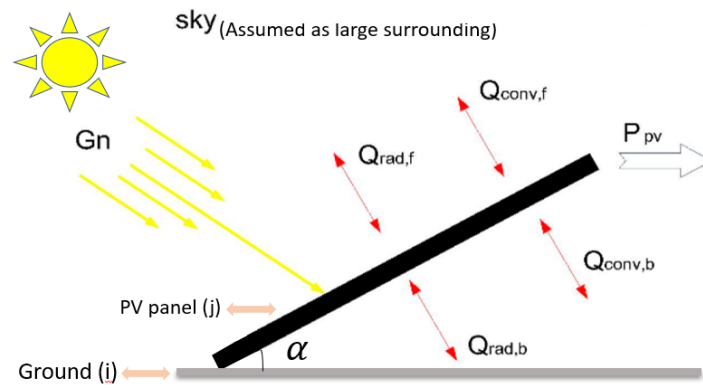


Figure 5.1: Consideration of energy types through the solar panel placed with the angle on the ground<sup>4</sup>. [33]

## 5.1 Energy Absorption by the PV Module

According to Figure 5.1:

$G_n$  is the solar irradiation to the solar panel ( $\text{W}/\text{m}^2$ ),

$G$  is the part of  $G_n$  absorbed into the PV module which is the sum of conductive heat ( $Q_{cond}$ ), convective heat and the electrical power generated in the PV panel.

The rest of  $G_n$  is reflected in the surrounding.

Assuming a steady state, the heat balance for the solar panel can be written as equation (5.2).

$$G - P_{pv} - Q_{total} = 0 \quad (5.2)$$

$$G = \delta G_n \quad (5.3)$$

Where in equation (5.3),  $\delta$  is the absorptivity of the surface depending on glass reflective properties. For more illustration equation (5.3) created by equations (5.4) to (5.7) which are as follows:

$$G = G_n A - G_{rif} A \quad (5.4)$$

$$G_{rif} = E = \rho G_n \quad (5.5)$$

$$P_{pv} = \eta G_n A \quad (5.6)$$

---

<sup>4</sup> The figure is modified according to the project model.

$$Q_{total} = Q_{conv,f} + Q_{rad,f} + Q_{conv,b} + Q_{rad,b} \quad (5.7)$$

The terms in Figure 5.1 and equations 5.4 to 5.7 described as:

$G_n$  is the sun irradiation on the solar panel front surface ( $\text{W}/\text{m}^2$ ),

$A$  is the surface area of the solar panel and should be considered to obtain the total power of the PV panel ( $\text{m}^2$ ),

$P_{pv}$  is the electrical power generated in the system ( $\text{W}/\text{m}^2$ ),

$\eta$  is the solar cell conversion efficiency that is 18.04 %, [19]

$G_{rif}$  is the total reflection from the solar panel ( $\text{W}/\text{m}^2$ ),

$\rho$  is the reflection index of the glass,

$Q_{total}$  is the total heat in the panel ( $\text{W}/\text{m}^2$ ),

Conductive heat inside the layers is lost by convection and radiation to the surrounding. Where:

$Q_{conv,f}$  and  $Q_{conv,b}$  are respectively the convective heat transfer rates of the front and pack of the panel with the surrounding ( $\text{W}/\text{m}^2$ ),

$Q_{rad,f}$  and  $Q_{rad,b}$  are radiative heat transfer of the front and back of the panel with the sky and ground respectively ( $\text{W}/\text{m}^2$ ),

Figure 5.2 can be a representative structure to the commercial solar panel JAM60S02-295/PR that consists of five layers in order as follows:

- Glass
- Ethylene Vinyl Acetate (EVA)
- Silicon semiconductor (PV cells)
- EVA
- Polyvinyl fluoride (PVF).

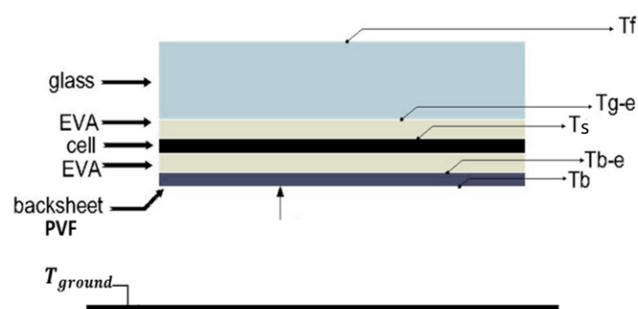


Figure 5.2: Solar panel layers material and temperature<sup>5</sup>. [33]

<sup>5</sup> The figure is modified according to solar panel JAM60S02-295/PR layers.

Temperatures in figure Figure 5.2 are:

$T_f$  is the front surface temperature (K),

$T_{g-e}$  is the temperature of the glass- EVA Contact surface (K),

$T_s$  is the temperature of the EVA- silicon contact surface (K),

$T_{b-e}$  is the temperature of the EVA- PVF contact surface (K),

$T_b$  is the temperature of the back sheet PVF (K),

The important properties of these materials are given in Table 5.1.

Table 5.1: Thermal conductivity, thickness and optical coefficients of the PV module layers. [13]

Material of layers	Thermal conductivity (W/(mK))	Thickness of material (m) [13]	Reflectivity ( $\rho$ )	transmissivity ( $\tau$ )	Absorptivity ( $\delta^6$ )
Glass (front)	$k_g = 0.98$	$L_g = 0.003$	0.1	0.88	0.02
EVA	$k_e = 0.23$	$L_e = 0.0004$	-	0.97	0.03
Silicon	$k_s = 148$	$L_s = 0.000018$	-	-	1
PVF (back)	$k_b = 0.36$	$L_b = 0.0005$	-	-	1

The emissivity of the bodies involved in radiation is given in Table 5.2.

Table 5.2: Emissivity of materials involved in radiation. [13] [43]

Material	Emissivity ( $\epsilon$ )
Black body	1
Glass surface of the solar panel	0.91
Clear Sky	0.91
Back of the solar cell (PVF)	0.85
Ground (Earth)	0.85
Water	0.95
Wood plane base	0.9

Thermal irradiation of sun is transmitted to all five layers of the solar panel as:

---

<sup>6</sup> Absorptivity symbol is typically shown by  $\alpha$ , but as it has been used for the solar panel angle, the absorptivity is shown by  $\delta$

- $G_1, G_2$  absorbed by the upper layers i.e. glass and EVA.
- All irradiation absorbed by the silicon layer is assumed to be power (when the circuit is connected to the power uptake source).
- $G_3, G_4$  absorbed by the bottom layers i.e. EVA and PVF.

The heat balance for each layer is written considering all heat as convection, conduction, radiation. In the third layer, electrical power is generated (heat is negligible). Considering absorption and transmission coefficients leads to equations (5.8) to (5.16).

$$G_1 = \delta_f G_n A \quad (5.8)$$

$$G_2 = \tau_f \delta_{EVA} G_n A \quad (5.9)$$

$$G_3 = \tau_f \tau_{EVA} (\delta_s K + \delta_{EVA}(1 - K)) G_n A \quad (5.10)$$

$$G_4 = \tau_f \tau_{EVA} \tau_{EVA} \delta_b (1 - K) G_n A \quad (5.11)$$

$$Q_{conv,f} + Q_{rad,f} - Q_{cond,g} + G_1 = 0 \quad (5.12)$$

$$Q_{cond,g} - Q_{cond,e1} + G_2 = 0 \quad (5.13)$$

$$Q_{cond,e1} - Q_{cond,e2} + G_3 - P_{pv} = 0 \quad (5.14)$$

$$Q_{cond,e2} - Q_{cond,b} + G_4 = 0 \quad (5.15)$$

$$-Q_{conv,b} - Q_{rad,b} + Q_{cond,b} = 0 \quad (5.16)$$

Where:

$A$  is the area of the solar panel ( $m^2$ ),

$\delta_f$  is absorptivity of the front surface (glass),

$\tau_f$  is the transmissivity of the front layer (glass),

$\delta_{EVA}$  is the absorptivity of EVA layers,

$\tau_{EVA}$  is the transmissivity of EVA,

$\delta_s$  is the absorptivity of the silicon PV cells layer,

$K$  is the ratio between the area of the silicon of the PV cells and the total area of the PV module which has been calculated as 0.901,

$\delta_b$  is the absorptivity of the back sheet (PVF),

Index  $f$  corresponds to the front panel surface,



Index  $b$  corresponds to the back surface of the panel (PVF),

$g$  corresponds to glass,

$e1$  to the first EVA layer,

$e2$  to the second EVA layer,

$PV$  to silicon PV cells. [33]

## 5.2 Heat Transfer Forms

The three forms of heat transfer have been described in the following chapters.

### 5.2.1 Radiation

For more illustration, equation (5.16) is the heat balance for the back surface of the solar panel when radiation from the ground should be considered. The two plates at the front are the front panel surface- sky and at the back are PVF layer- ground.

If the base is wood or water instead of ground, the emissivity of wood or water should be considered. Radiative heat exchange between two parallel plates, assuming the same area for both plates, is obtained by equations (5.17) and (5.18).

$$Q_{rad} = h_{rad} A (T_1^4 - T_2^4) \quad (5.17)$$

$$h_{rad} = \frac{\sigma}{\frac{1 - \varepsilon_1}{\varepsilon_1} + \frac{1}{F_{12}} + \frac{1 - \varepsilon_2}{\varepsilon_2}} \quad (5.18)$$

Where:

$T_1$  and  $T_2$  are the surface temperatures of front surface- sky or back surface- ground (K).

$h_{rad}$  is the heat transfer coefficient of radiation ( $W/m^2K^4$ ),

$\sigma$  is Stephan- Boltzmann constant  $5.67 \times 10^{-8} W/(m^2K^4)$ ,

The emissivity of involved materials is given in Table 5.2. [33]

$F_{12}$  is called the view factor which is equal to unity for two parallel plates. But if the plates are placed with angle, the view factor is not equal to unity due to the view angle as can be seen in Figure 5.1 shows the geometry of angled plates. Equation (5.19) is used to calculate the view factor of angled plates. Then can be inserted in equation (5.18) to calculate radiative heat exchange.

$$F_{ij} = 1 - \sin\left(\frac{\alpha}{2}\right) \quad (5.19)$$

Where  $F_{ij}$  is the view factor of  $i$  and  $j$  plates,

$\alpha$  is the angle between plate  $i$  and plate  $j$ . [29]

### 5.2.2 Conduction

Conductive heat transfer through solar panel layers can be calculated to obtain the temperature change in each layer. Thus, the following procedure leads to having the conductive heat transfer or temperature of each layer.

According to Figure 5.2, as the area of all layers is constant and equal, conductive heat flux through the panel can be considered constant so equations (5.20) to (5.26) illustrate the calculation procedure from the front panel surface to the back of the panel.

$$Q''_{cond} = \frac{Q_{cond}}{A} = h_{rad,f} (T_f^4 - T_{a,f}^4) + \bar{h}_{conv,f} (T_f - T_{a,f}) \quad (5.20)$$

Where:

$h_{rad,f}$  is the radiative heat transfer coefficient at the front panel  $W/m^2K^4$ ,

$\bar{h}_{conv,f}$  is the average convective heat transfer coefficient at the front panel ( $W/m^2K$ ),

$T_{a,f}$  is the temperature of the air at the front panel (K).

For the following equations, thermal conductivity and thickness are given in Table 5.1.

$$Q''_{cond} = \frac{k_g}{L_g} (T_f - T_{g-e}) \quad (5.21)$$

$$Q''_{cond} = \frac{k_e}{L_e} (T_{g-e} - T_{e-s}) \quad (5.22)$$

$$Q''_{cond} = \frac{k_s}{L_s} (T_{e-s} - T_{s-e}) \quad (5.23)$$

$$Q''_{cond} = \frac{k_e}{L_e} (T_{s-e} - T_{e-b}) \quad (5.24)$$

$$Q''_{cond} = \frac{k_b}{L_b} (T_{e-b} - T_b) \quad (5.25)$$

$$Q''_{cond} = h_{rad,b} (T_b^4 - T_{a,b}^4) + \bar{h}_{conv,b} (T_b - T_{a,b}) \quad (5.26)$$

Where:

$T_{g-e}$  is the temperature of the glass-EVA contact surface,

$T_{e-s}$  is the temperature of the EVA-Silicon contact surface,

$T_{s-e}$  is the temperature of the Silicon- EVA contact surface,

$T_{e-b}$  is the temperature of the EVA-PVF contact surface,

$h_{rad,b}$  is the radiative heat transfer coefficient at the back of the panel,

$\bar{h}_{conv,b}$  is the average convective heat transfer coefficient at the back of the panel,

$T_{a,b}$  is the temperature of the air at the back of the panel,

The summation of equations (5.20) to (5.26) leads to the final equation (5.27).

$$Q''_{cond} = \frac{h_{rad,f}(T_f^4 - T_{a,f}^4) + \bar{h}_{conv,f}(T_f - T_{a,f}) + h_{rad,b}(T_b^4 - T_{a,b}^4) + \bar{h}_{conv,b}(T_b - T_{a,b}) + (T_f - T_b)}{2 + \frac{L_g}{k_g} + 2\frac{L_e}{k_e} + \frac{L_s}{k_s} + \frac{L_b}{k_b}} \quad (5.27)$$

Temperatures can be read from the data logger sensors.

### 5.2.3 Convection

The terms affecting the convective and radiative heat transfer coefficients are air temperature, ground temperature, wind speed, the temperature of the PV module, the geometry and the angle of the PV module.

Nusselt number is the determining factor of heat transfer coefficient in convection. The speed of wind determines laminar or turbulent conditions around the panel.

In this system, the assumption is both the front and back of the panel have the same turbulent or laminar conditions. According to the ambient conditions, Nusselt number is dependent on Reynolds number (Re), Prandtl number (Pr), Rayleigh number (Ra) and Grashof number. The convective heat transfer rate is given in equation (5.28).

$$Q_{conv} = \bar{h}_{conv} A (T_{surface} - T_a) \quad (5.28)$$

Equation (5.29) shows the average heat transfer coefficient for the whole area of the panel.  $L_c$  (m) this equation corresponds to the characteristic length of the PV module (Area/perimeter).

$$\bar{h}_{conv} = \frac{Nu k}{L_c} \quad (5.29)$$

Being:

$\bar{h}_{conv}$  the convective coefficient (W/(m<sup>2</sup>K)).

A heat transfer area (m<sup>2</sup>).

$\Delta T$  the temperature difference between the surface and the surrounding temperature (K).

$k$  is the thermal conductivity of the air around the PV module (W/(mK)).

$Nu$  is the dimensionless Nusselt number. [29]

Equations (5.30) to (5.33) show the other dimensionless numbers that are used in calculating the Nusselt number.

$$\text{Pr} = \frac{\nu}{\chi} \quad (5.30)$$

$$\text{Gr} = \frac{g \beta (T_s - T_a) L_{ch}^3}{\nu^2} \quad (5.31)$$

$$\text{Ra} = \text{Gr Pr} = \frac{g \beta (T_s - T_a) L_{ch}^3}{\nu \chi} \quad (5.32)$$

$$\text{Re} = \frac{u_a L_{ch}}{\nu} \quad (5.33)$$

Prandtl number represents information about the type of fluid in reference conditions. The amount of Prandtl number for fluids can be found in tables in heat transfer books. Moreover, it gives information about the thickness of the thermal boundary layer and hydrodynamic properties of the boundary layer.

Grashof number indicates the relation between heat and mass transfer of a solid which has been immersed in a fluid and natural convection occurs between them due to temperature difference.

Reynolds number corresponds to the dominance of viscous or inertial forces on the fluid around the surface of the PV module to determine laminar, turbulent or mixed conditions. The Rayleigh number which is determined by Grashof and Prandtl numbers is a definition of the relation between momentum diffusivity and thermal diffusivity. All these numbers are unitless. [33]

In equations (5.30) to (5.33):

$\nu$  is the dynamic viscosity ( $\text{m}^2/\text{s}$ ).

$\chi^7$  is thermal diffusivity ( $\text{m}^2/\text{s}$ ).

$g$  is gravity acceleration ( $\text{m}/\text{s}^2$ ).

$u$  is the air or wind speed.

$\beta = 1/T$  is isobaric compression ratio ( $1/\text{K}$ ).

The reference temperature to identify the above parameters is the film temperature which is shown in equation (5.34).

$$T_{ref} = \frac{T_a + T_s}{2} \quad (5.34)$$

---

<sup>7</sup> Thermal diffusivity is typically shown by  $\alpha$ , but since it is used as the angle of the solar panel, the symbol  $\chi$  is used for thermal diffusivity.

$T_a$  (K) corresponds to the free stream temperature around the PV surface.

$T_s$  (K) corresponds to the temperature of the PV panel surface (front or back).

In order to select the correct formula to calculate the Nusselt number, the main consideration is to see the flow conditions. The transition from laminar to turbulent conditions occurs in the critical Reynolds number which is defined as  $Re_c$  meaning that the laminar and turbulent length can be found by using this number.

For the PV module geometry, a flat plate,  $Re_c = 5 \times 10^5$ . For laminar condition, Reynold's number of the fluid is less than  $Re_c$  and for turbulent conditions, it is higher.

There is a critical number for Rayleigh and Grashof number. Based on the information from the weather station, the airflow can be determined as laminar, turbulent or mix of both for the entire PV panel. [29]

#### 5.2.4 Panel in Horizontal Position

Calculation of average Nusselt number can be done based on the geometry and the position of the solar panel which is considered as an isothermal flat plate. For horizontal position and laminar condition, equation (5.35) can be used to calculate the average Nusselt number at any position in the x-direction.

$$\overline{Nu}_{x,forced} = \frac{\bar{h}_x x}{k} = 0.664 Re_x^{1/2} Pr^{1/3} \quad Pr \geq 0.6 \quad (5.35)$$

As following, for horizontal position and turbulent condition equation (5.36) to (5.38) can be used to obtain average coefficients based on the fact that turbulent condition generally occurs after laminar boundary layer so in order to have more precision a mixed boundary condition is considered.

$$\bar{h}_L = \frac{1}{L} \left( \int_0^{x_c} h_{lam} dx + \int_{x_c}^L h_{turb} dx \right) \quad (5.36)$$

Where  $0 \leq x \leq x_c$  is the laminar region and  $x_c \leq x \leq L$  corresponds to the turbulent region.

$$A = 0.037 Re_c^{4/5} - 0.664 Re_c^{1/2} \quad (5.37)$$

$$\overline{Nu}_{L,forced} = (0.037 Re_L^{4/5} - A) Pr^{1/3} \quad (5.38)$$

$$\left[ \begin{array}{l} 0.6 \leq Pr \leq 60 \\ Re_x \leq Re_L \leq 10^8 \end{array} \right]$$

Where:

$Re_x$  indicates the Reynolds number at position  $x$ ,

$Re_L$  indicates the Reynold number of the entire length of the plate,

For completely turbulent conditions  $A = 0$  and for the transition Reynold number for a flat plate  $A = 871$ . All properties are evaluated at  $T_{ref}$ . [29]

### 5.2.5 The panel in Angled Position

If the PV panel is mounted with an angle to the base, inclined plates correlations should be used to calculate the average Nusselt number given in equations (5.39).

When calculating the Nusselt number for the back of the panel, the speed of air interferes with the inclined plates the gravity in the Rayleigh number equation should be corrected by  $g \cos(\theta)$  to consider the effect of the angle.

$$\overline{Nu}_{L,natural} = \left\{ 0.825 + \frac{0.387 (Ra_L \cos(\theta))^{1/6}}{[1 + (0.492/Pr)^{9/16}]^{8/27}} \right\}^2 \quad (5.39)$$

Forced or natural convection or mixed convection is determined by the proportion of Grashof to Reynold number, as:

- $Gr/Re^2 \sim 1$  corresponds to mixed convection.
- $Gr/Re^2 \gg 1$  shows natural convection.
- $Gr/Re^2 \ll 1$  represents the forced convection.

When mix condition is dominant and natural convection occurs in the opposite of forced convection, equation (5.40) is used to obtain the correct Nusselt number.

$$Nu = \sqrt[3]{(Nu_{L,natural})^3 + (Nu_{L,forced})^3} \quad (5.40)$$

[33]

## 6 Simulation

In the simulation chapter, simulating the power generation, the heat balance and DC/AC inverter of the solar panel are described.

### 6.1 Simulation the Power Generation

Simulation of PV systems can be done with simulating software such as MATLAB/Simulink, Lab View, LT SPICE from Linear Technology company or other software.

The simulation is done with MATLAB/Simulink because it has good features for PV modeling and DC/AC converter. Also, most of the simulations on P-V and I-V curve analyses are done with this software. In order to model the heat balance, Simulink has a thermal library for heat transfer. In addition, the Simscape electrical library can be used for DC/AC inverter. Thus, Simulink is chosen as the simulation software for this project. [44]

#### 6.1.1 Assumptions

Assumptions for the simulation are:

- Steady-state conditions.
- No shading effects

Parameter values for simulation are acquired from electrical parameters in the solar panel datasheet.

#### 6.1.2 Constant Parameters

Initial values are defined as Table 6.1 in model properties.

Table 6.1: Initial parameters for the simulation. [19]

Parameter	Value	Parameter	Value
Diode ideality factor	$n = 1.1$	Boltzmann constant	$k = 1.38 \times 10^{-23} \text{ A}$
Current coefficient <sup>8</sup>	$K_I = 0.0006$	Electron charge	$q = 1.6 \times 10^{-19}$
Bandgap energy in the semiconductor	$E_g = 1.5 \text{ e V}$	Number of cells in series	$N_s = 60$
Series resistance	$R_s = 0.221 \Omega$	Parallel resistance	$R_p = 414.5 \Omega$

In order to make the model, five main equations such as photovoltaic current, saturation current, reverse saturation current, the current passing the shunt resistor and total output current is used.

---

<sup>8</sup> Current coefficient is the short-circuit current of the PV cell at STC (25 °C and 1000 W/m<sup>2</sup>)

First, the simulation is done for STC conditions:

- $T = 25\text{ }^{\circ}\text{C}$  and  $G = 1000\text{ W}$ .
- $V = 32.03\text{ V}$  and  $I = 9.21\text{ A}$  at maximum power.
- $V_{oc} = 39.64\text{ V}$ ,  $I_{sc} = 9.66\text{ A}$  was used in the model to find maximum power that is rated as  $P = 295\text{ W}$ .

At NOCT:

- $G = 800\text{ W/m}^2$  and  $T_a = 20\text{ }^{\circ}\text{C}$ .
- The maximum voltage giving the maximum power is  $V_{mp} = 29.63\text{ V}$ .
- The current at maximum power is  $I_{mp} = 7.32\text{ A}$ .
- $V_{oc} = 36.57\text{ V}$ ,  $I_{sc} = 7.69\text{ A}$  and maximum power is  $217\text{ W}$ .

The PV panel consists of the number of PV cells. In JAM60S02-295/PR solar panel, every 20 PV cells which are connected in series, have a parallel connection with one diode according to the solar panel design. Then the diodes of adjacent groups connect in series.

That means the current in each cell is equal to the total current in PV panel and the total voltage created in the PV panel is the sum of the voltage in each cell.

### 6.1.3 Power Generation in Simulink

The inputs for power generation are air temperature and solar irradiation. The temperature can be obtained by weather station application or any other weather application.

For real conditions and real data, using information in Table 6.1: Initial parameters for the simulation. [19]Table 6.1, with the angle of the panel gives the estimated total irradiation for different seasons and different weather. Another database to obtain solar irradiation on earth is the weather station website.

For STC conditions the angle of the panel is assumed as zero, meaning that the panel is horizontally mounted. The effect of angle is considered in calculating the solar irradiation on the solar panel.

Connecting blocks used in the simulation were constant, add, subtract, product, input, output, XY graph, out.sim and ramp. The whole simulated system can be seen in Figure 6.1.

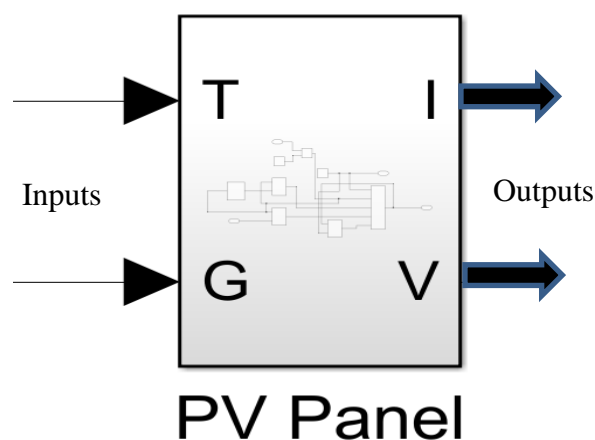


Figure 6.1: The overall diagram of the PV panel in Simulink.



In order to obtain I-V and P-V curves, five main equations of the single-diode model are used; saturation current equation, reverse saturation current equation, photovoltaic current equation, shunt resistor current and finally the solar panel output current. All these equations are described completely in chapter 4.

The inputs can be air temperature and solar irradiation, while the outputs are voltage and current of the solar panel. The reverse saturation current block is made as shown in Figure 6.2.

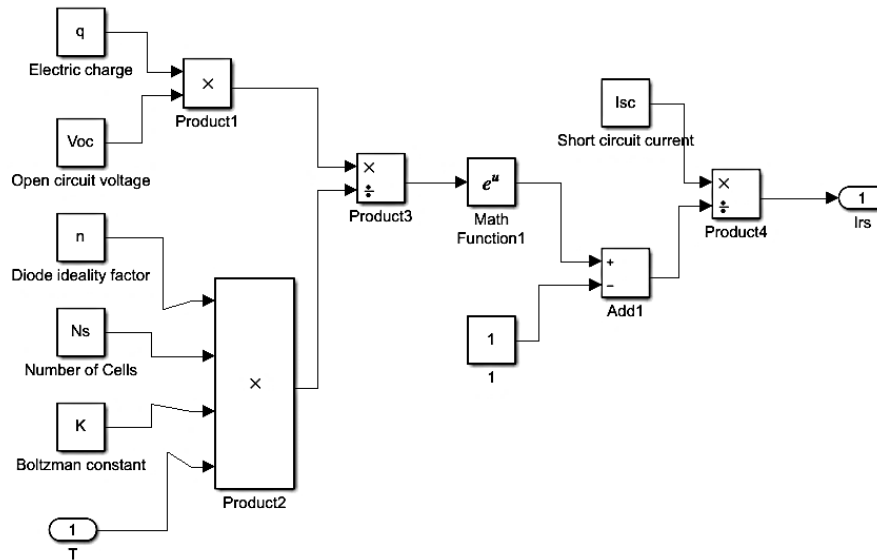


Figure 6.2: The reverse saturation current block.

The reverse saturation current is made as an input to calculate the saturation current. Figure 6.3 shows the saturation current block.

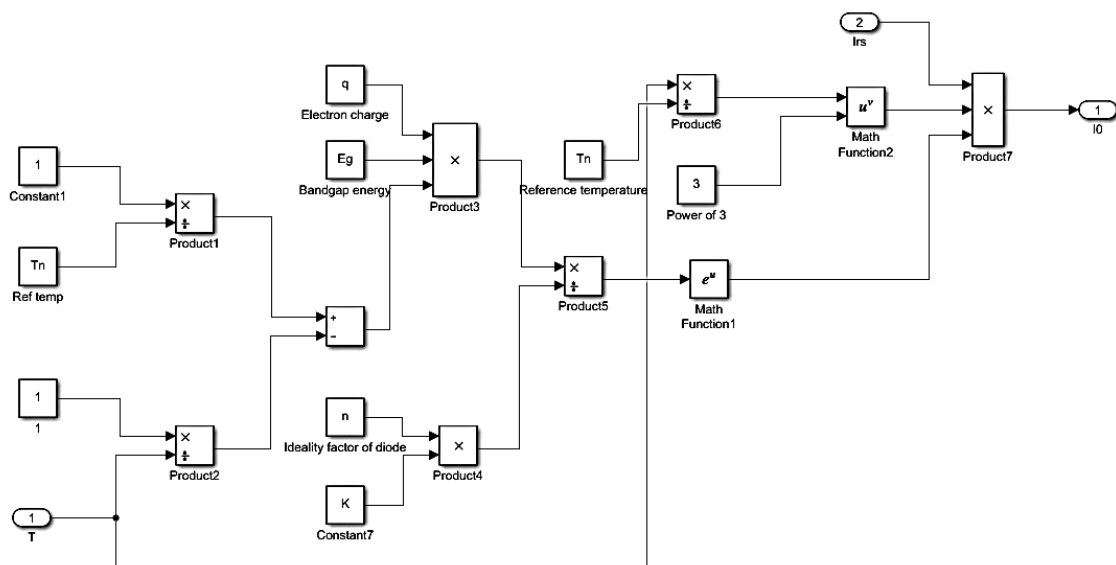


Figure 6.3: Saturation current block.

The ambient temperature and irradiation are inputs to photovoltaic current. Their block is given in Figure 6.4.

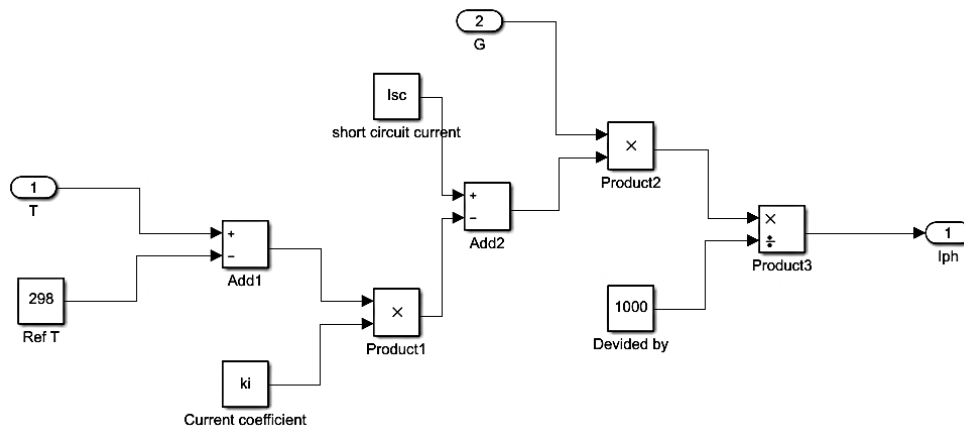


Figure 6.4: The block of photovoltaic current.

The shunt resistance block is made as shown in Figure 6.5.

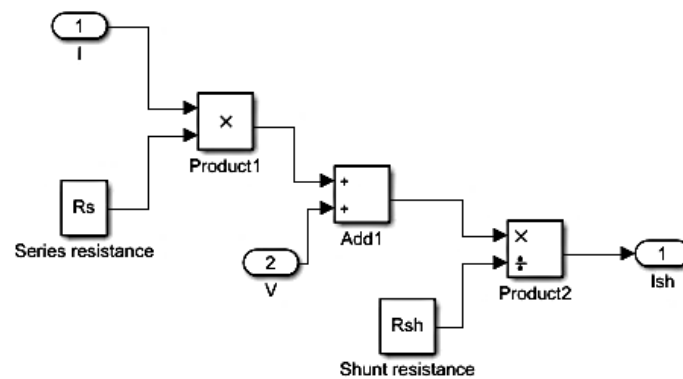


Figure 6.5: Shunt resistance block.

All the blocks shown in Figure 6.2 to Figure 6.5 are connected as shown in Figure 6.6. All the connections to each block can be seen.

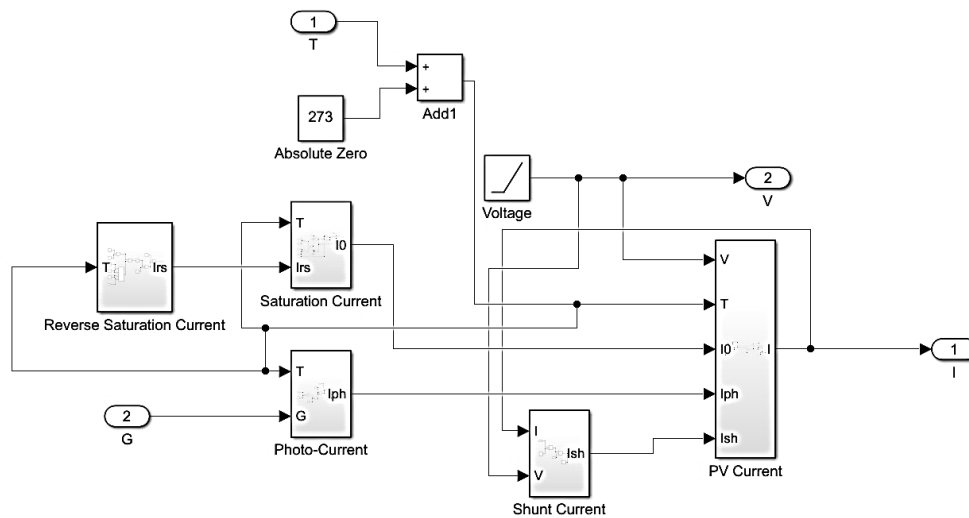


Figure 6.6: Connection of current blocks to ultimate I and V.

The final system can be seen in Figure 6.7. I-V and P-V graphs are inserted to obtain such curves for the solar panel. All the required constants are defined in the model parameters.

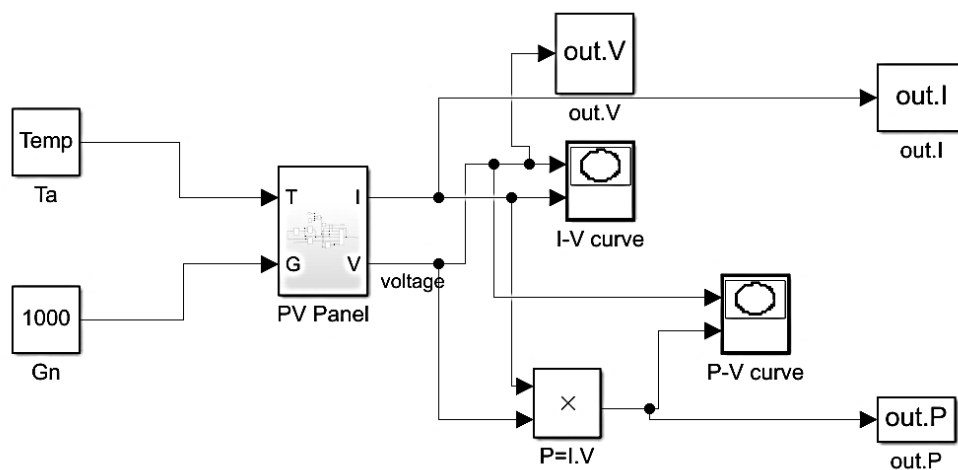


Figure 6.7: The final block diagram of the model in Simulink.

The running time for the simulation was 4 seconds. In order to obtain better graphs for comparison, a MATLAB code is written to have the plots corresponding to every 3 temperatures in every figure. The MATLAB code is shown in Figure 6.8.

```

Temp_ar= [-2.,5.,10.];
I_ar=zeros(length(Temp_ar),21)
V_ar=zeros(length(Temp_ar),21)
P_ar=zeros(length(Temp_ar),21)
for i=1:length(Temp_ar)
    Temp=Temp_ar(i);
    out=sim('SolarpanelPV')
    I_ar(i,:)=out.I';
    P_ar(i,:)=out.P';
    V_ar(i,:)=out.V';
end

figure(1)
hold on
title('P-V curve & I-V curve')
subplot(2,1,1);
for i=1:length(Temp_ar)
    plot(V_ar(i,:),P_ar(i,:))
    hold on
end

xlabel('Voltage')
ylabel('Power')
ylim([0,5])
legend('Temp=-2','Temp=5','Temp=10')
subplot(2,1,2);
for i=1:length(Temp_ar)
    plot(V_ar(i,:),I_ar(i,:))
    hold on
end
xlabel('Voltage')
ylabel('Current')
ylim([0,2])
legend('Temp=-2','Temp=5','Temp=10')
A1=max(P_ar);
Ma_A=max(A1);

```

Figure 6.8: Connecting the MATLAB code with Simulink to give its input and make multiple plots.

This code is used to give temperatures as inputs and see the I-V, P-V curves in one figure. Temperatures can be changed in the code, then running the program. The absorbed irradiation can be changed according to real conditions in the Simulink program directly.

## 6.2 Heat balance Simulation

The heat balance modeling to predict the temperature of each layer was done with the thermal and fluid library in Simulink library which was downloaded via the Add-Ons options in MATLAB. These libraries have blocks for heat transfer equations and thermometers. [45]

### 6.2.1 Assumptions

In order to make a representative model estimates the temperature increase of the solar panel, the following assumptions are made:

- Steady-state conditions meaning that the changes of temperature by time is constant.
- The system has five layers with conduction, two surfaces with convection and irradiation
- All over the layer is isothermal.

- Heat transfer occurs in one dimension and the system is isotropic.
- Constant thermal and physical properties for solar panel layers.
- The constant emissivity of the PV panel layers being independent of temperature and wavelength.
- The radiation coefficients such as reflection ( $\rho$ ), transmission ( $\tau$ ) and absorption ( $\delta$ ) are independent of temperature.
- No internal reflection between the layers of the solar panel. [29] [33]

### 6.2.2 Parameters

The area of the solar panel can be found from solar panel specifications in Table 2.1 as:

$$A = 1.650 \times 0.991 \text{ m}^2 = 1.63515 \text{ m}^2$$

Convective and radiative heat transfer coefficients should be calculated with values from tables in heat transfer books. Due to obtaining parameters based on real conditions, the temperatures of the panel, ground and surrounding air is used from the data logger. The average air temperature is read from the weather station. [29]

The irradiation is measured by the spectrometer or read from the weather station. Weather station irradiation gives the normal irradiation to the ground and is multiplied by the cosine panel angle.

### 6.2.3 Heat Balance for Closed-Circuit

Heat balance simulation is done considering:

- Closed- circuit, the solar panel is exposed to sun and the panel is connected by wires to a power uptake source.
- The silicon layer only produces power and it is a transparent layer. This means the heat generation is neglected for the silicon layer.

The blocks used for the simulation are convective, conductive, radiative heat transfer elements, Simulink unit convertor, heat flow element, thermal source element, constant blocks, add, subtract, product blocks and temperature source elements.

The overall Simulink block connections for a closed-circuit is shown in Figure 6.9. As can be seen, radiative and convective thermal elements are defined for the surface and the back of the panel. Five layers are considered with five conductive heat transfer elements. Irradiance absorbance is considered for the two upper layers and the two bottom layers. Temperatures corresponding to each layer are set as Kelvin (K) unit.

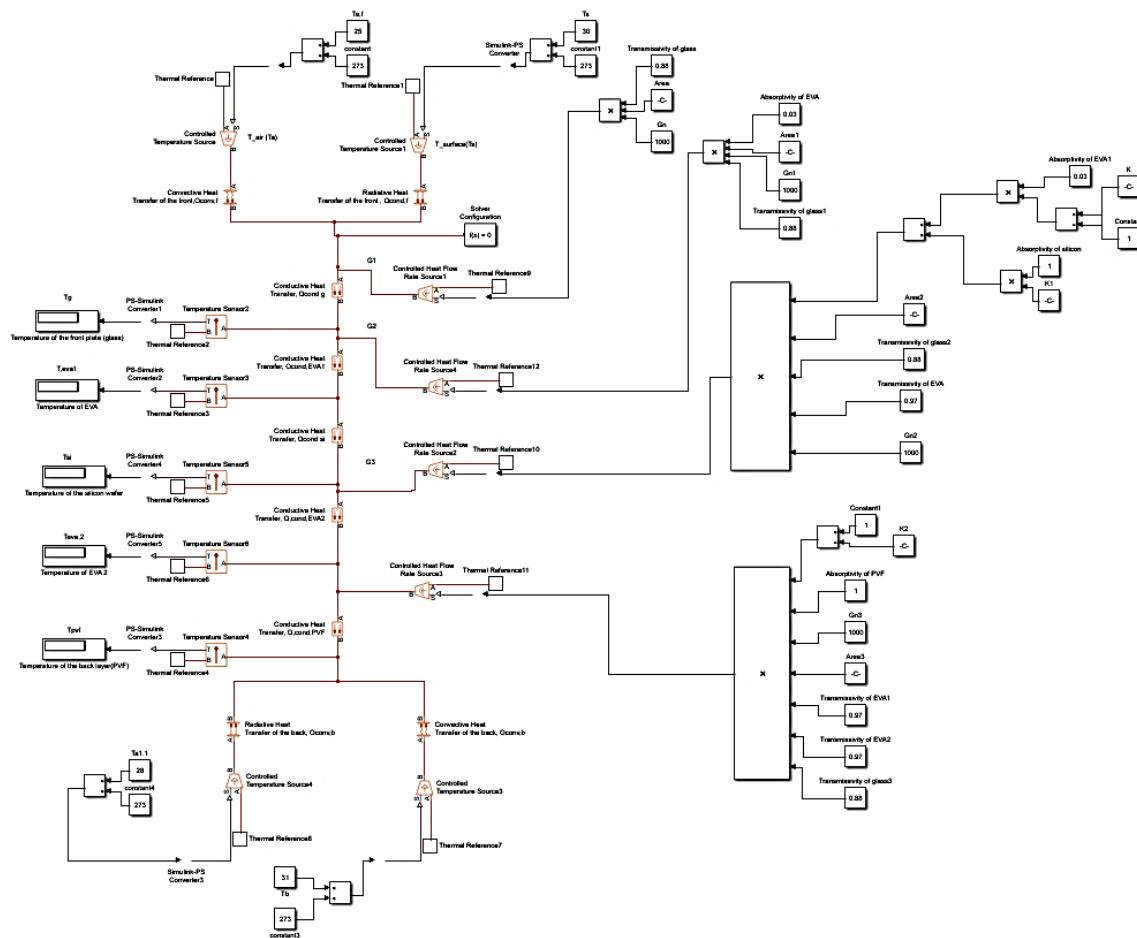


Figure 6.9: Applied heat balance model for a closed-circuit solar panel.

The effect of radiation between the ground and back is considered in calculating the radiative heat transfer coefficient for the back of the panel.

#### 6.2.4 Heat Balance for Open-Circuit

Simulation when the panel is exposed to sunlight, but no wires are connected, is done to see how the power is dissipated if there is no power uptake. In order to show that in the simulation, an input equal to the maximum power generation is added to the third layer to see temperature changes in the layers.

The power is added as a constant heat flow element to the block which is connected to the conduction part of the third layer. The added term and the placement are shown in Figure 6.10 with a line around it.

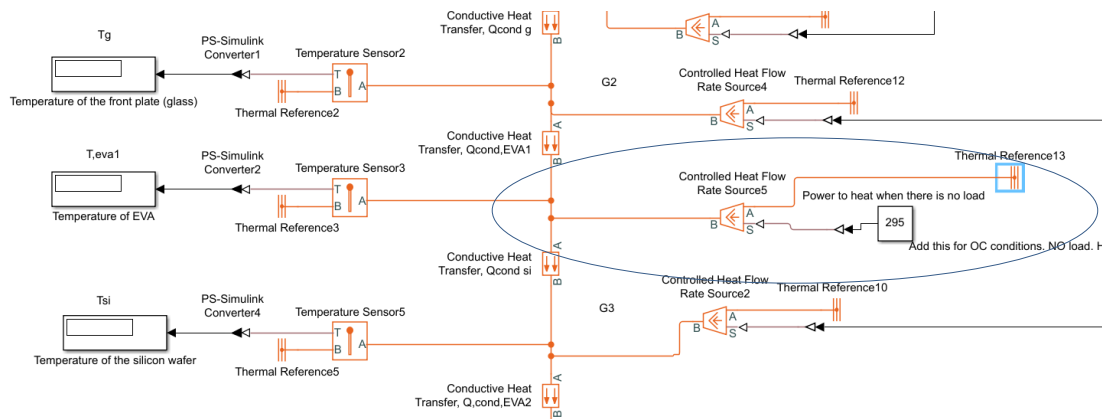


Figure 6.10: Heat balance for open circuit solar panel exposed to the sun.

### 6.2.5 Shading Effects

Shading effects in the simulation can be done for power generation and heat balance as:

- Reducing the area of the solar panel which can represent the irradiation area and reduction of the number of the cells.
- Consider an upper layer over the glass with different absorptivity and transmissivity, which can be the different thickness of snow or dust.

To apply these changes in the simulation, the values of corresponding parameters should be changed.

## 6.3 DC/AC Inverter

To have a better illustration of true sine wave inverters which are the most efficient types of investors. A simple single-phase DC/AC conversion is done.

The blocks are used from Simscape electric library containing PV array, DC voltage source, pulse generator, IGBT/diodes semiconductors, series RLC branches, continuous powergui, voltage measurement, and scope. [44]

### 6.3.1 Parameters

Since no real inverter was available, assumed values are used for the DC/AC inverter part. The PV array is set for a single solar panel with the same values as the power generation part. For amplitude, time delay and resistance, assumed values are inserted.

### 6.3.2 Model in Simulink

The simulation is done as shown in Figure 6.11. The run time is set to 0.1 s. The converted sine wave can be seen in the scope block. The principle is when the pulse generator is run, it opens the two IGBT conductors that are connected to it. After this cycle is finished, the second pulse generator starts running and switches its two connected IGBT conductors on. These alternating pulses continue until the end of the running time. This continuous cycle generates alternating sine waves. RLC resistances are used to show a smooth dissipation and oscillation during the runtime.

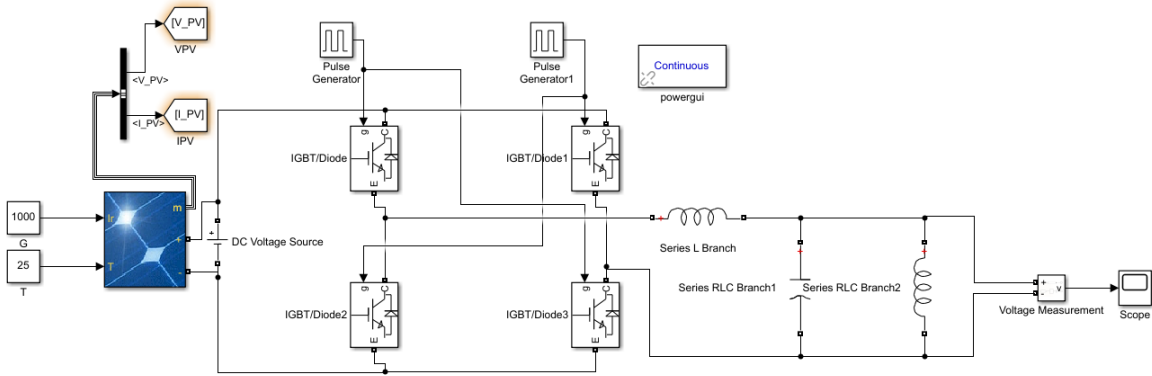


Figure 6.11: Simulation of DC/AC inverter.



## 7 Application for Weather Station

Weather station data such as air temperature, wind speed, and solar irradiation are required for simulation. The parameters from the weather station can be read directly from the server. The following chapter gives an overview of the weather station system and the development of the weather data saving application.

### 7.1 Weather Station Description

The weather station placed on the C building at USN Campus Porsgrunn is from Colombia Weather Systems and consists of Capricorn 2000EX Weather Station, sensors and The Weather MicroServer. Figure 7.1 shows the weather station system. The control module and Weather MicroServer is described in the following chapters. The network router, LAN, SQL server Express and LabVIEW, and cloud database are related to the data storage.

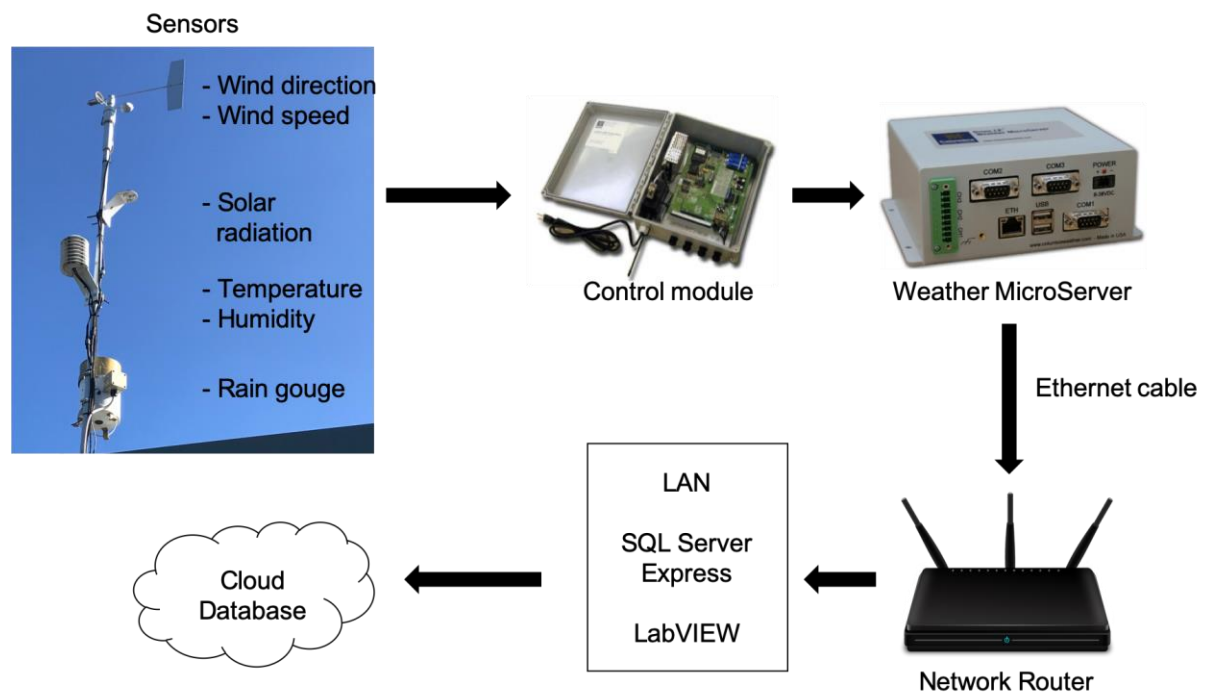


Figure 7.1: A sketch of the weather station system, with sensors, Control module, Weather MicroServer, Ethernet cable, Network Router, LAN and the cloud database. Sketch made with figures from [46] [47, 48]

#### 7.1.1 Capricorn 2000EX Weather Station

The Capricorn 2000EX Weather Station contains the control module and sensors. The control module includes a data storage marked with date and time. In addition, the max/min information is stored at user-defined intervals. The Dual onboard RS-232 interfaces allow connection to a display console, modem, or directly to a computer at the same time. [49]

The sensors featured in this weather station are wind direction and speed, solar radiation, temperature, humidity and rain gauge. For this project, only the wind direction and speed, solar radiation and temperature is relevant. The wind sensors are made of durable aluminum/stainless

steel. The speed sensor is rated up to 160 MPH and the wind direction sensor provides greater resolution and accuracy. [49]

A precision potentiometer is used for the wind direction sensor, while a sealed reed switch is used for the wind speed sensor. The solar radiation (or pyranometer) sensor is calibrated to measure the shortwave radiation reaching the earth's surface. This is measured in watts per m<sup>2</sup>. To prevent water accumulation the sensor is dome-shaped. It is also self-cleaning and potted solid to prevent condensation. The temperature sensor is a digital, semiconductor probe, calibrated at the factory. It is possible to connect up to four temperature sensors. [49]

### 7.1.2 The Weather MicroServer

The weather MicroServer is an independent proprietary system using the Linux operating system. The server produces an "internet-ready" weather monitoring system by automatically providing FTP output, XML web service, and Internet browser user interface. With the Weather MicroServer, data logging is a possibility. It can be connected to a network using an Ethernet cable. It also provides real-time weather data. This gives the user the possibility to monitor the weather at any computer connected to the network. [46]

## 7.2 Automatic Data Collection from the Weather Station

In order to collect data from the weather station, the data reading system should be connected to the ethernet connection in the university to have the accessibility to the given IP-Address. Having connected to the ethernet connection and providing the necessary authentication, the real-time data can be read from the global website, as it is shown in Figure 7.2.

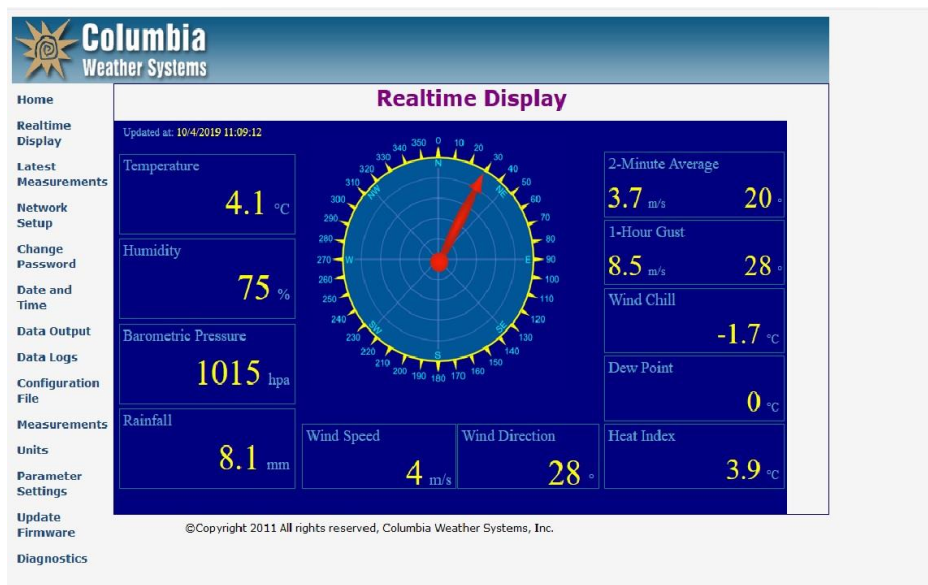


Figure 7.2: The screenshot taken of real-time data at a specific date and time.

For collecting data from the weather station, the reader needs to be connected to the server for every single reading. This makes collecting data a challenging task for every collection. However, by automating the data collection using the LabView ModBus library, the system automatically collects data every time that the receiver got connected to the server.

In Figure 7.3, the overall sketch of the application for the weather station can be seen. In the first step, the client (Master) can be connected to the server (Slave) by the ModBus protocol with given TCP or the IP address.

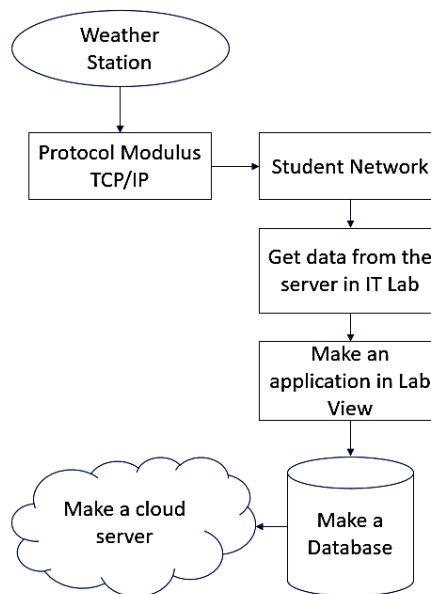


Figure 7.3 Sketch of Data automation steps

## 7.3 Developing the Application to Save Weather Station Data

In order to have communication from the server with the program, the communication can be executed by the ModBus protocol or directly by the XML file. A short review of the ModBus protocol is presented in this section.

### 7.3.1 ModBus protocol

The ModBus protocol uses master and slave architecture. The master transmits a request to a slave and the slave responds. This gives the master full control over the information. This request is a layered set of data, where the application data unit (ADU) is the first layer. This is to most people considered to be the “type” of ModBus used. TCP/IP, ASCII, and remote terminal unit (RTU) are the three types of ADUs. Figure 7.4 shows the relation between the master and the slave [50].

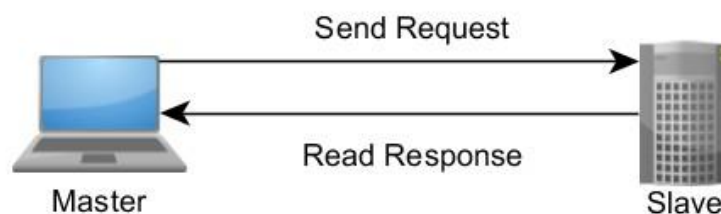


Figure 7.4: The master-slave relation of the ModBus protocol. [50]

### 7.3.2 Developing the application

The MicroServer weather station works with ModBus TCP mode for making the request and reading data from the sensor. In this sense, the LabView has a library called ModBus capable of requesting reading data from the server, as it is shown in Figure 7.5.

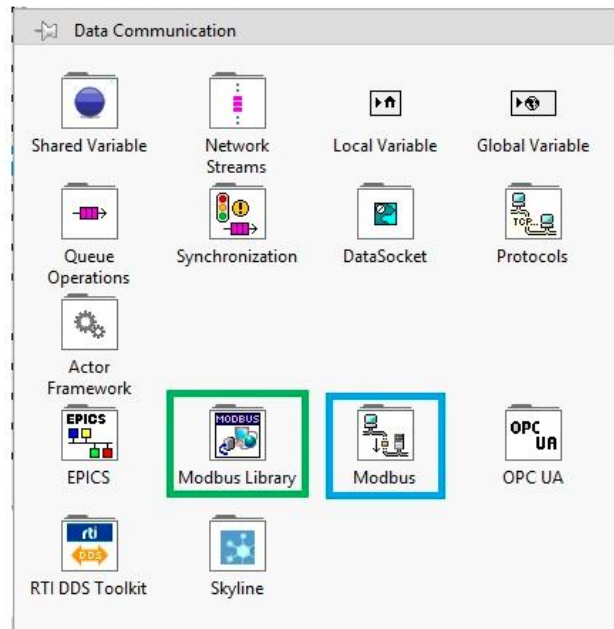


Figure 7.5: Screenshot of the ModBus Library and ModBus in the LabView program

The reading system as the client, or the master, requests the server to read the data and the server gives the client the required data. With the LabView application, it can be done to write a program based on the master TCP client with the given IP address and requesting the registered input value for each sensor. The data which are read are unjustified raw 16-bit figured which have to be converted to the right amount with the offset and factor for every parameter, which are given in the weather station manual. In Figure 7.6, the basic form of the application which is capable of acquiring data from the weather station is shown.

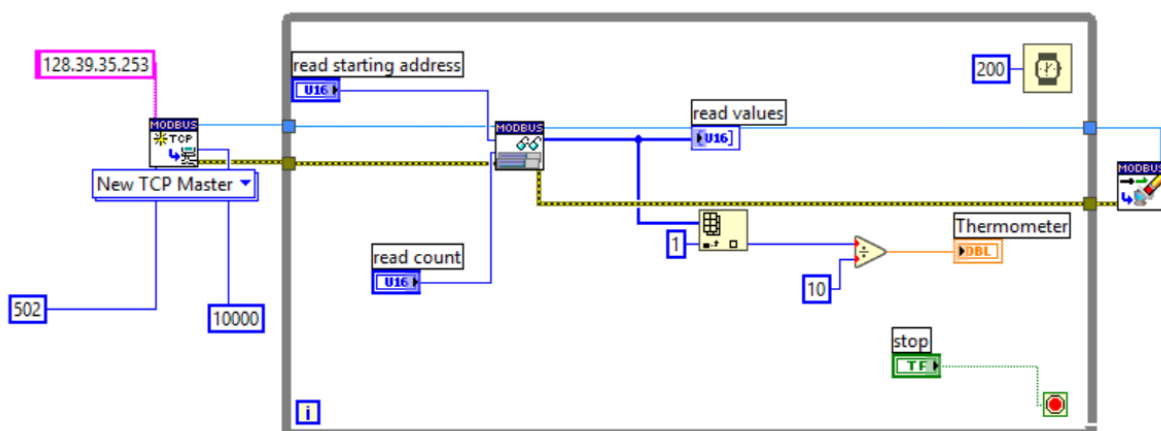


Figure 7.6: Program in Lab View to get data from the weather station.

In this application, first, a TCP Master box is created in order to get access to the local host, then the IP address of the host is given. As it is given from the manual and the weather station resources, the IP address for the weather station to get access via the ethernet connection in the university is 128.39.395.253 with the port number of 502. A reading application from the ModBus library is created to read data. In this icon, the input registry of each section and sensor needs to be addressed. However, all data that are going to be read are in the form of 16 or 32-bit unjustified numbers which give the client different values from those in the real-time. In order to justify all those data, a conversion of data should be done. With the given formula in equation 7.1, the unjustified data will be converted to the real data which corresponds to the exact number of temperature other parameters.

$$\text{Parameter value} = (\text{unsigned 16-bit integer} + \text{offset}) / \text{factor} \quad (7.1)$$

In the weather station manual, every offset and factor for each factor is given and it needs to be put in the application in order to get the real data from the server.

For example, for the temperature the offset is -17920 and the factor is 256. Consequently, for a data which the unjustified number is equal to 27080, the real value for the temperature with using equation (7.1) would be approximately 35.78°F. After the conversion from Fahrenheit to Celsius, the temperature is 2.1°C, which is correspond to the real value of the day it was recorded.

The next thing for the storing data is automatic data storing. In this sense, a program needs to be developed to get the data every day automatically. An application needs to be developed corresponds to the main program which collect the data from the LabView every time with or without using the application at the time. Finally, all measured data will be stored in a database created in the SQL server to collect all of them in one table. In the Figure 7.7, the collected data at the specific date and time in the created database is shown.

	Date_Time	Temperature_C	Wind_Speed_...	Wind_Direction	Humidity	Barometric_Pr...
	2019-11-14 18:1...	3.1	1.8	321	83	1009
	2019-11-14 18:1...	3.1	2.2	28	83	1010
	2019-11-14 18:2...	3.1	3.1	6	83	1010
	2019-11-14 18:2...	3.1	3.6	22	83	1010
	2019-11-14 18:2...	3.2	3.6	332	83	1010
	2019-11-14 18:2...	3.2	1.3	118	83	1010
	2019-11-14 18:2...	3.2	1.3	51	83	1010
	2019-11-14 18:3...	3.2	3.1	22	83	1010
	2019-11-14 18:3...	3.2	2.2	287	83	1010
	2019-11-14 18:3...	3.2	2.2	287	83	1010
	2019-11-14 18:3...	3.2	2.2	321	83	1010
	2019-11-14 18:3...	3.1	3.6	332	83	1010
	2019-11-14 18:4...	3.1	2.2	298	83	1010
	2019-11-14 18:4...	3.1	1.8	17	83	1010
	2019-11-14 18:4...	3.1	1.3	79	83	1010
	2019-11-14 18:4...	3.1	1.3	343	83	1010
	2019-11-14 18:4...	3.2	1.3	270	83	1010
	2019-11-14 18:5...	3.1	1.3	270	83	1010
	2019-11-14 18:5...	3.1	0.9	73	83	1010
	2019-11-14 18:5...	3.1	0.9	56	83	1010

Figure 7.7: The screenshot from the table in SQL for collecting stored data from the weather station application

After storing measured data in the database, the final step is to save them in a cloud storage. The main advantage of storing data in a virtualized database, namely cloud storage, is feasibility of getting access to that information for everyone via different locations or using multiple computers.

In the chapter11, the progress and difficulty of developing a cloud database only for this purpose and automatic saving will be discussed.

# 8 Practical Experiment

This chapter is about setting up the solar panel to do outdoor measurements. In addition, setting up the data capture and control software are described.

## 8.1 Requirements

In order to have outdoor test measurements, the 4 additional devices which are described in chapter 2, are used as follows:

- Solar panel from JAM60S02-295/PR
- Electronic load GWINSTEK PEL 3031E in order to measure the current, voltage and power.
- Data logger Grant 2020 series is used to measure 4 temperatures of front panel, back of the panel.
- Spectrometer Model CXR-SR in order to measure the sun irradiation.
- Capricorn 2000EX Weather Station system for solar irradiation and wind speed.
- A computer with an internet connection, all required software installed on it.

Every instrument has its specific software. It is required to use the following software to get solar data and save them:

- LinkView [LINKVIEW-B] VER 1.10023 for the electronic load.
- Squirrel view to read data from the data logger.
- SpectraWiz to get irradiation data.

Additionally, software which is required data storage is:

- The Microsoft SQL server v18.3 was used to make the basic tables and databases for both the weather station and the solar panel measurements.

## 8.2 Setting Up Devices and Connections

Outdoor measurements were done in order to have real data to complete the following parts:

- Calculation the solar panel layer temperatures with real data.
- Make the order of tables in a database.

The panel was taken out to have measurements, the connections to the solar panel are shown in Figure 8.1.



Figure 8.1: Solar panel set up and connections.

The air sensor is kept close to the panel to measure the surrounding air temperature. The ground sensor is dug into the ground under the panel. The front and back temperature sensors are stuck to the surface and back of the panel respectively.

### 8.3 Software Set up and Operation

The software is used to control and get data from the load module, data logger and spectrometer are described at the following.

#### 8.3.1 Set Up LinkView

As described in chapter 2, the electronic load is connected via USB to a computer port. Figure 8.2 shows the setup of LinkView. The connection port number is found in the windows device manager. The number of computer port and channel is inserted as shown in the figure. There is no electronic power supply, so no channel is defined for the power supply. When the device is connected, a successful connection message appears.

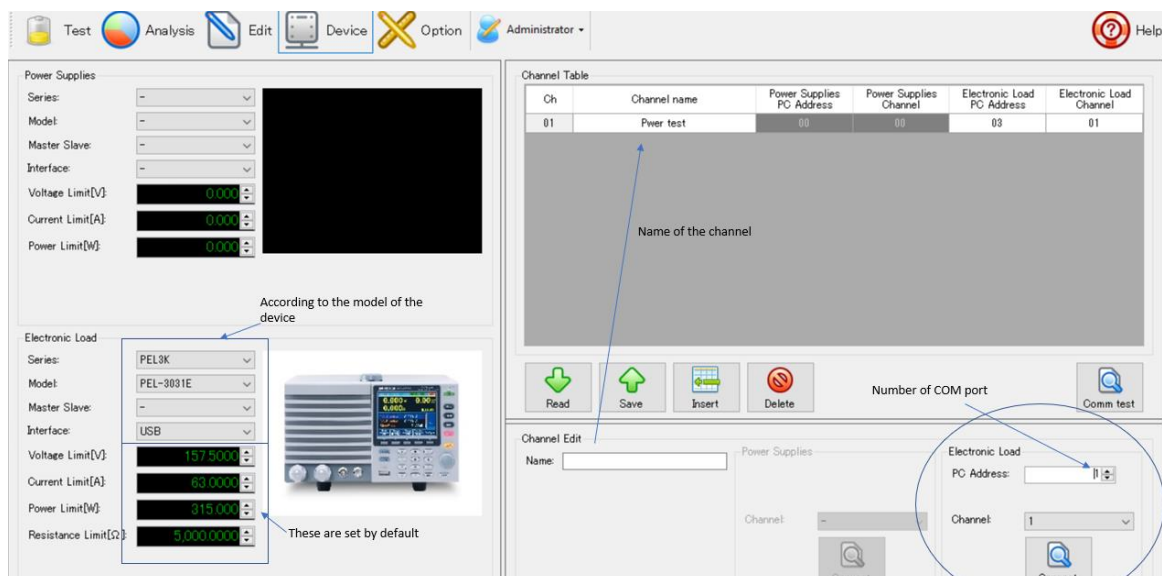


Figure 8.2: The environment and LinkView set up.



Realterm software is another option to control GWinstek 3031E remotely. Data from Realterm is saved as CSV Excel. Realterm should be run as an administrator, then the connection port is set in the port section.

The display window is set to Ascii. After setting the port properties, the computer is connected to the device, the connection status is shown in the right bottom corner as shown in Figure 8.3 and three bottoms to the right called Ring, CTS, DSR blink with green color. [51]

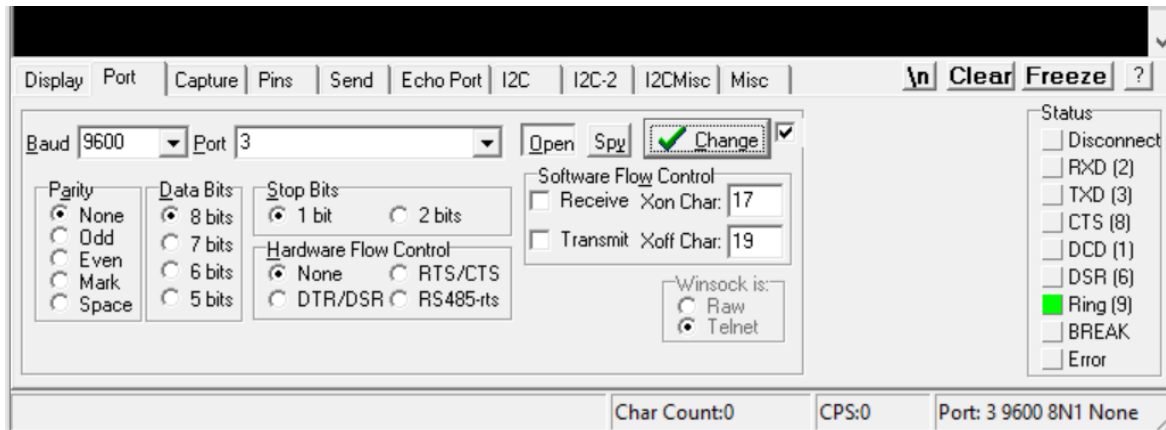


Figure 8.3: Set up the port section in Realterm. Baud, port, parity, bits are set. The right bottom corner shows the port is connected.

In the send display, the command ‘\*idn?’ is written in the EOL part with check-marking +CR, +LF. If the electronic load is connected to the device, the specific number and version of the device are shown in the Realterm command window.

In order to capture data, a new capture file as.CSV type is defined in the capture part. By clicking the Start: Overview button, electronic load data should be captured. This version of electronic load only supports connection to Windows Vista, XP, 7 and 8.

Connecting two software to one port is not possible. If the LinkView is open and connected to the port, Realterm or other capturing software cannot capture data.

Another option to control the electronic load remotely is GPIB port that connects the device to a Lab View application. However, the LabView application cannot be used for this device version because it lacks GPIB port.

### 8.3.2 Set Up Squirrel View

A software named Squirrelview is used to read the data collected from the temperature sensors. This is offered by Grant instruments. This program gives easy setup of the logger, fast download of data and easy export to excel files. The software has a communication wizard so working with modems, ethernet, GMS, and Wireless systems is straight forward. By using MS scheduler, downloader for automating tasks is possible when Squirrelview Plus used. [52]

The logger setup is shown in Figure 8.4. The sensor type, a description of what the sensor is measuring, connections and log method was added for the right block (A, B and D). Then the logger was armed, and the temperatures was measured.

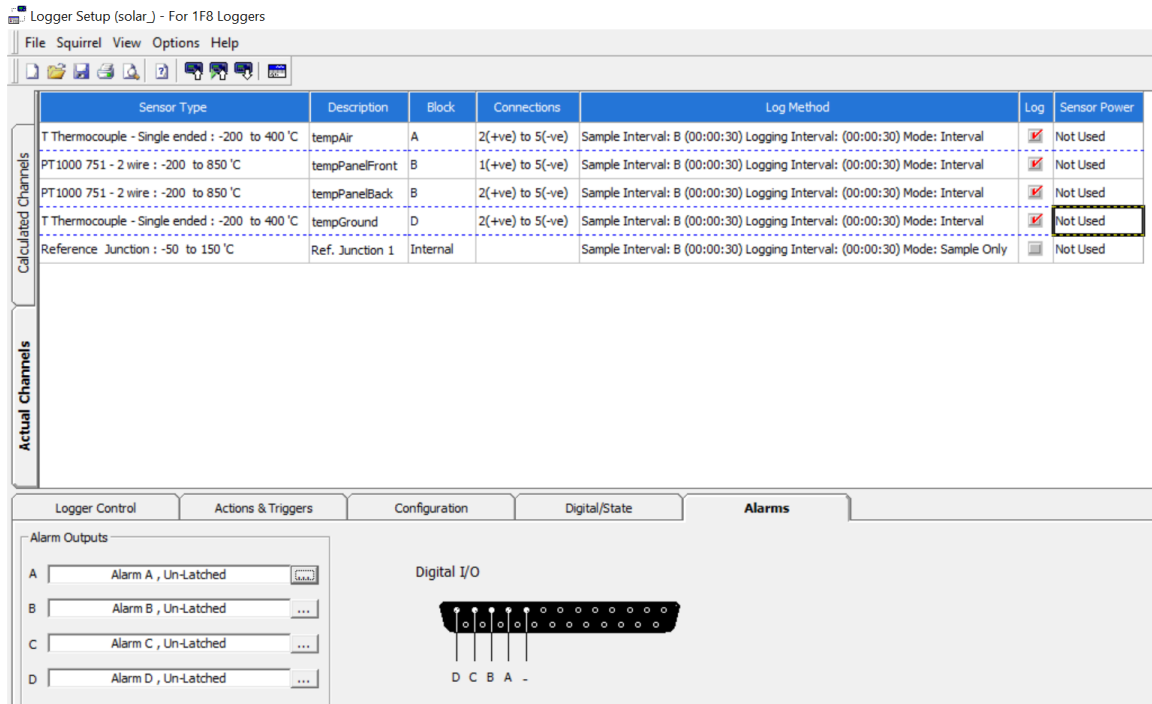


Figure 8.4: A screenshot of the logger setup for solar panel temperature measurements.

### 8.3.3 Set Up SpectraWiz

SpectraWiz Spectroscopy Software is StellarNet's main software program for its spectrometers and is included for every spectrometer. There are several options for use of SpectraWiz. It is compatible with mobile apps, LabView, Mac OS, Python, MATLAB and Haze. The independent SpectraWiz Software can be used to display wavelengths and radiation within each wavelength area for different light sources. For solar panels, this can be used to compare effects from sunlight and artificial sunlight. [53]

By using LabView with SpectraWiz it rapidly customizes the software to be used in any application. The features include all instrument configuration parameters, spectral data in scope mode, irradiance mode, absorbance mode, and transmission mode. LabView can show wavelengths as a function of time and export the data to files. This is very useful for the measurements of solar radiation while working with the solar panel. [53]

The use of SpectraWiz in this project is for collecting data from the sunlight received by the solar panel. For every measurement from the spectrometer, there must be created a baseline. This baseline is a dark spectrum and is critical for the accuracy of the measurements. Because of limited time and resources for this project it will not be possible to make an automation of the baseline. This limits the measuring capacity as the baseline should be made for every temperature change. The manual procedure for creating a baseline is to cover the sensor of the spectrometer until it does not receive any light and save the curve.

For the use of SpectraWiz in this project, the program itself provides the necessary measurements. SpectraWiz measures the wavelength and radiance. Considering the use of manual baseline and no measurements of sunlight on the roof, SpectraWiz itself is sufficient for this project.

For automatic data saving from the spectrometer, SpectraWiz for LabView is required. This software is independent of the SpectraWiz program. A set up with the spectrometer and LabView was made, but the program failed to connect with the spectrometer. Because of this,

the program is suggested to be used in further work when more features are necessary. It is assumed that automatic data saving and an automatic baseline program could be made. This is out of the competence of this project considering only energy and process engineers are involved.

The measurements and data acquired from SpectraWiz should be compared to the ASTM Reference Spectra shown in Figure 8.5. This spectrum shows the solar spectral irradiance in the atmosphere on a specific surface and is used as a standard table for irradiance measurements. The standard has also an Excel spreadsheet to compare data more accurately. [54]

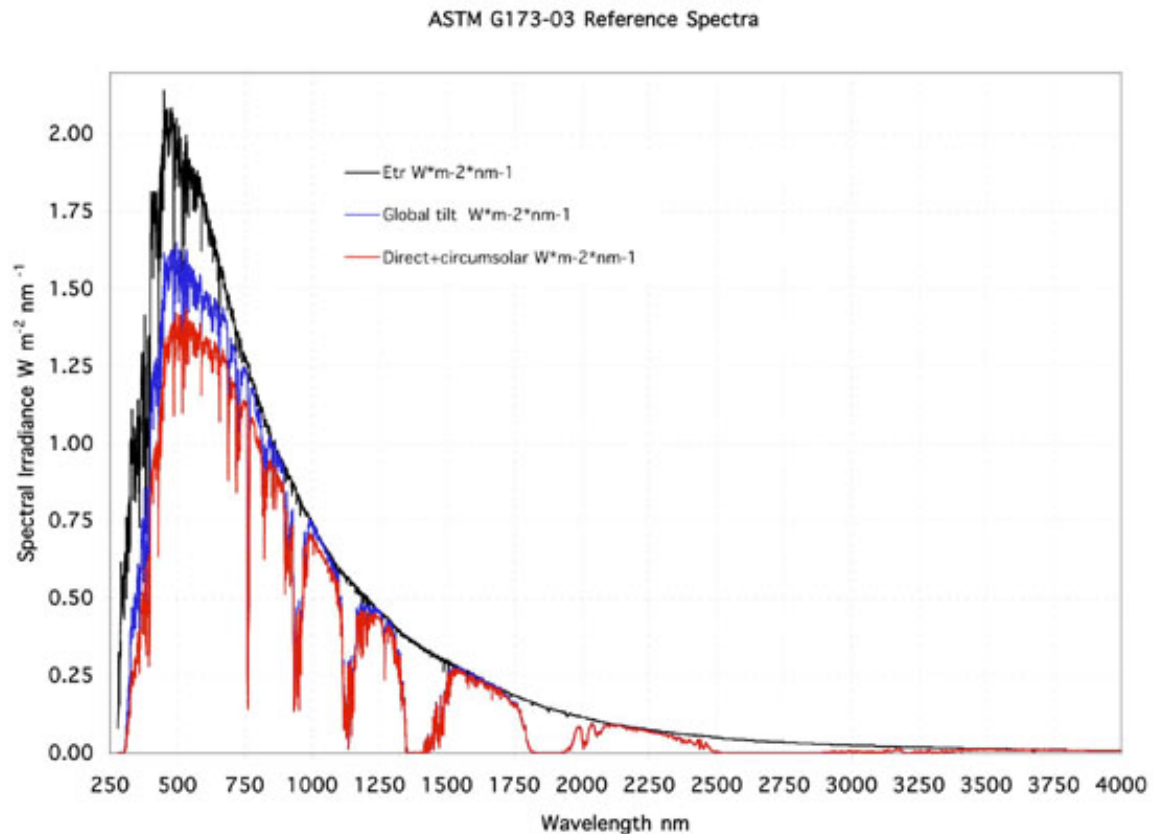


Figure 8.5: Standard curve for solar spectral irradiance. [54]

## 8.4 Mounting the Panel on the Roof

Figure 8.6 shows the probable sketch of mounting the solar panel.

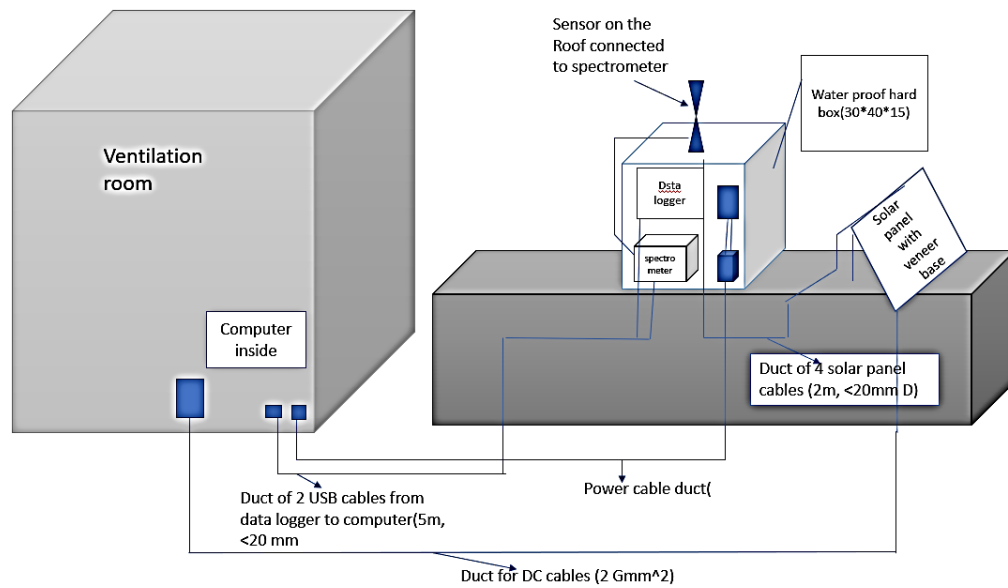


Figure 8.6: Sketch of mounting solar panel outdoor on the roof of a building.

The box for the spectrometer, electronic load, and data logger should be a waterproof box with enough insulation properties to be resistant to freezing in winters. The solar panel cables should be in a waterproof antifreeze duct. Another consideration is to choose the cost effective materials satisfactory to the budget.

## 9 Data Collection

This chapter is about outdoor measurements with solar panel, data saving procedure, the possibilities or procedures of automatic data saving.

### 9.1 Electrical Data Collection

Data collection from the electronic load needs defining mode sequences. For PEL-3031E, the operating limits should be considered in order to set the sequences:

- High range: Voltage 0-60, current 0-150.
- Low range: voltage 0-150 V, current 0-6 A.
- Low current range in operating mode for DC measurements: voltage 1 V, 6 A.
- High current range in operating mode for DC measurements: voltage 1 V, 60 A.

The solar panel generates direct current (DC) power. The sequences in LinkView should be in an acceptable range. Accordingly, four patterns are defined for the electronic load in order to find the correct mode to measure the generated power. As shown in Figure 9.1, pattern test1 is defined as sleep, constant current, constant resistance, constant voltage, constant power running one after another with one repeat. The sleep mode is to calibrate the measurements. All the parameters such as resistance and current are kept as the default setting. The voltage range is set on high voltage.

Pattern Edit														
No: 001		Name: test1										Repeat: 1		
Step Table														
No	Mode	Parameter	Time[S]	End Condition						Error Detection				
				Voltage[V]		Current[A]		Power[W]		Voltage[V]		Current[A]		
				Hi	Lo	Hi	Lo	Hi	Lo	Hi	Lo	Hi	Lo	
001	Sleep	-	60	OFF	OFF	OFF	OFF	OFF	OFF	OFF	OFF	OFF	OFF	OFF
002	Discharge CC	H, 0.000A	60	OFF	OFF	OFF	OFF	OFF	OFF	OFF	OFF	OFF	OFF	OFF
003	Discharge CR	H, 0.016Ω	60	OFF	0.000	OFF	0.000	OFF	OFF	OFF	OFF	OFF	OFF	OFF
004	Discharge CV	H, 1.000V	60	OFF	0.000	OFF	0.000	OFF	OFF	OFF	OFF	OFF	OFF	OFF
005	Discharge CP	H, 0.000W	60	OFF	0.000	OFF	0.000	OFF	OFF	OFF	OFF	OFF	OFF	OFF

Figure 9.1: Pattern test1 to measure power with the electronic load.

The second pattern test 2 is set as shown in Figure 9.2. It is seen that the steps are sleep, then seven constant voltage modes with different measuring ranges and 5 seconds running time for each step.

Pattern Edit

No: 002 Name: custrant voltage rise Repeat: 1

Step Table

No	Mode	Parameter	Time[S]	End Condition						Error Detection				
				Voltage[V]		Current[A]		Power[W]		Voltage[V]		Current[A]		
				Hi	Lo	Hi	Lo	Hi	Lo	Hi	Lo	Hi	Lo	
001	Sleep	-	20	OFF	OFF	OFF	OFF	OFF	OFF	OFF	OFF	OFF	OFF	OFF
002	Discharge CV	H, 1.000V	5	OFF	1.000	OFF	OFF	OFF	OFF	OFF	OFF	OFF	OFF	OFF
003	Discharge CV	H, 5.000V	5	OFF	5.000	OFF	OFF	OFF	OFF	OFF	OFF	OFF	OFF	OFF
004	Discharge CV	H, 10.000V	5	OFF	10.000	OFF	OFF	OFF	OFF	OFF	OFF	OFF	OFF	OFF
005	Discharge CV	H, 15.000V	5	OFF	15.000	OFF	OFF	OFF	OFF	OFF	OFF	OFF	OFF	OFF
006	Discharge CV	H, 20.000V	5	OFF	20.000	OFF	OFF	OFF	OFF	OFF	OFF	OFF	OFF	OFF
007	Discharge CV	H, 25.000V	5	OFF	25.000	OFF	OFF	OFF	OFF	OFF	OFF	OFF	OFF	OFF
008	Discharge CV	H, 35.000V	5	OFF	35.000	OFF	OFF	OFF	OFF	OFF	OFF	OFF	OFF	OFF

Figure 9.2: Pattern test 2 to measure power with the electronic load.

Test 3 is set as shown in Figure 9.3. One step of constant power is set for 5 seconds in this test.

Pattern Edit

No: 003 Name: load 1 Repeat: 1

Step Table

No	Mode	Parameter	Time[S]	End Condition						Error Detection				
				Voltage[V]		Current[A]		Power[W]		Voltage[V]		Current[A]		
				Hi	Lo	Hi	Lo	Hi	Lo	Hi	Lo	Hi	Lo	
001	Discharge CP	-, 0.000W	5	OFF	OFF	OFF	OFF	OFF	OFF	40.000	OFF	OFF	OFF	OFF

Figure 9.3: Pattern test 3 to measure power with the electronic load.

Pattern test 4 is set to 5 steps of sleep, and 3 constant currents with 10 seconds running time and low current ranges as seen in Figure 9.4.

Pattern Edit

No: 004 Name: current steps Repeat: 1

Step Table

No	Mode	Parameter	Time[S]	End Condition						Error Detection				
				Voltage[V]		Current[A]		Power[W]		Voltage[V]		Current[A]		
				Hi	Lo	Hi	Lo	Hi	Lo	Hi	Lo	Hi	Lo	
001	Sleep	-	5	OFF	OFF	OFF	OFF	OFF	OFF	OFF	OFF	OFF	OFF	OFF
002	Discharge CC	L, 0.001A	10	OFF	OFF	OFF	OFF	OFF	OFF	OFF	OFF	OFF	OFF	OFF
003	Discharge CC	L, 0.002A	10	OFF	OFF	OFF	OFF	OFF	OFF	OFF	OFF	OFF	OFF	OFF
004	Discharge CC	L, 0.100A	10	OFF	OFF	OFF	OFF	OFF	OFF	OFF	OFF	OFF	OFF	OFF

Figure 9.4: Pattern test 4 to measure power with the electronic load.

These sequences are used for outdoor testing. Up to 101 patterns can be saved in the software. the sequences are executed by clicking start, then commanded to the electronic load. The correct sequence will show values for voltage, current, and power.

The LinkView software is able to import and export files to a local folder in the computer, but it is usable in older Microsoft WINDOWS versions as vista, XP, 7 and 8. Another possibility is printing measured values according to real-time.

Another program called Serial Port Monitor is tested, but the only connection occurred between the program and the computer port. It showed zero data and did not capture any measurement.

## 9.2 Temperature Data Collection

To get the data, a CSV file is manually downloaded in the Squirrelview assistant panel. Click on the 'download data' button and choose what data to be downloaded, and where to save it. It is also important to choose export in the 'action after download' option. The download can be done while the logger is armed, and it will continue to measure until it is disarmed in the 'logger control' at the assistant panel.

To save the data from the data logger automatic the Squirrelview plus software is used with Microsoft Scheduler Tasks. To set up the automatic data download, run the Downloader Control Panel. A window with two split halves will appear. The profile pane with the names of all the profiles that have been created is located on the left side. The right side is the data pane, which contains all the settings for a given profile. To schedule a download a few steps need to be completed. First make sure the Downloader Control Panel is running, then right-click on the profiles in the profile pane that is used to create the schedule. Then choose 'create/Edit Task (Microsoft Scheduled Tasks)'. A new window will appear. Click on the Schedule tab and select 'New'. Here the time and date of the for the required schedule are added. Then click 'OK'. When the password is confirmed, the downloader will run at the scheduled time. [55]

## 9.3 Irradiance Data Collection

For the irradiance data collection, the spectrometer and SpectraWiz were used. The spectrometer was connected to the computer and the sensor. The sensor was set up in the open window with the approximately same angle as the solar panel. To create the dark spectrum, the sensor was covered and the spectrum saved. Then the wavelength could be measured. To avoid the curve from being saturated, the integration time can be increased. The first curve shows the raw data from the sun. This is the amount of photons versus light in the nanometer. To get irradiation per  $W/m^2$ , the program needs to be changed at View-Radiometer and then choose Watts. When the curves are stabilized the data can be saved and converted into excel. Screenshots were taken of the curves as well.

# 10 Database

In this chapter, the general idea of database and Microsoft SQL server for managing the database is described. In addition, the cloud database for storing data in a virtualized environment will be covered. The created databases both for the solar panel measurement and the weather station are presented in addition to how tables collect data from those resources.

## 10.1 Description of Database and Cloud Storage

The database is a set of data or information that can easily be organized, managed and updated when it needed to add or adjust data. There are different kind of databases such as relational databases, distributed databases, cloud databases and other types.

One of the main relational interfaces working with the databases is the Microsoft Standard Query Language (SQL). Microsoft SQL server is a relational database management system developed by Microsoft. As a database server, it is a software product with the primary function of storing and retrieving data as requested by other software applications—which may run either on the same computer or on another computer across a network (including the Internet). [56]

Having collected data from the resources, which in this project are solar panel systems and the weather station, and putting them into a database, the next step is to develop a cloud storage for storing data into a virtualized environment. Cloud storage is a service model where digital data are stored in logical pools. [56]

In this project, two different databases are set for two main programs. One is for all data collected from the solar panel and the other one is the database for the weather station. The program used for making the database is Microsoft SQL server V18.3.

## 10.2 Developing a Database in Microsoft SQL Server

The overall environment of the SQL management studio in which a database can be created is shown in Figure 10.1.

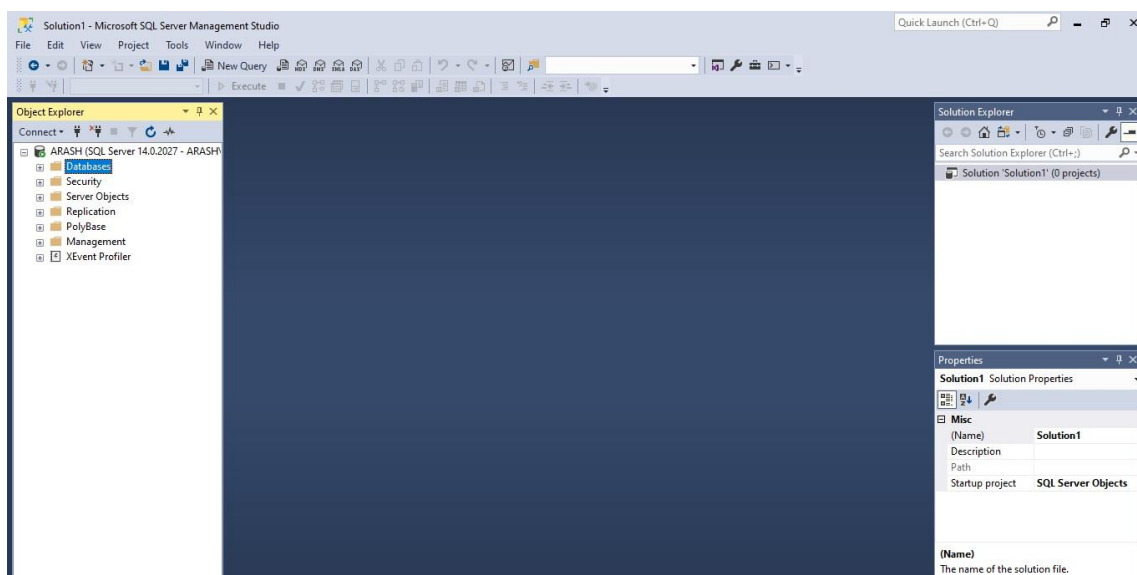


Figure 10.1: A screenshot from the visual management studio.



For every database which is needed to be created, in the left menu, it can be added, and all required data or information can be added to different tables.

### 10.3 Database for the Weather Station

In the weather system in which different data such as temperature, wind speed, and other important parameters are going to be read, a database is needed to sort out to write and record different data from different times and dates.

In this case, firstly a LabView application has been developed to collect the required data from the weather station with a specific IP address. Sequentially, with a link from LabView to Microsoft SQL server, all the information imported to the database which is created for this purpose. Figure 10.2 shows some of the parameters read by the LabView from the weather station in the SQL table.

	WeatherParam...	ParameterName	Unit	ModbusAddress	ModbusName
▶	4	Temperature	Celsius	30037	Temp1
	6	WindSpeed	m/s	30005	WindSpeed
	10	WindDirection	Degree	30009	WindDir
	11	Humidity	%	30017	RelHumidity
	1011	BarometricPres...	hpa	30025	BaromPress
	1012	Irradiation	GW	30035	Irrad
*	NULL	NULL	NULL	NULL	NULL

Figure 10.2: The weather station parameters in the SQL server

Having created the primary table for the weather station values, a link from LabView to SQL was developed to import data from the stored file in the LabView to the SQL server. After the importing is implemented, a table designed for this case will appear to show all data stored in the database.

### 10.4 Database for Solar Panel Measurements

Same as the weather station system, a database for solar panel measurement has been created for each device. The data were read at different dates and times and were imported into an excel file or CSV file where they can be inserted into the desired database in the SQL server.

As described in previous chapter 9, the data from the load transfer were measured via GWINSTEK PEL-3031 and the result was saved as in a Microsoft excel file. In order to insert data into the database, the stored data were imported as a flat-file into the Microsoft SQL server, as it is shown in Figure 10.3.

Date_2019	Time	Channel	Step	Run_Time_s	Voltage_value_V	Current_value_A	Power_W
2019-11-07 00:0...	11:00:01	1	1/4	00:00:01	38.272	0	0
2019-11-07 00:0...	11:00:02	1	1/4	00:00:02	38.272	0	0
2019-11-07 00:0...	11:00:03	1	1/4	00:00:03	38.282	0	0
2019-11-07 00:0...	11:00:04	1	1/4	00:00:04	38.392	0	0
2019-11-07 00:0...	11:00:05	1	1/4	00:00:05	38.492	0	0
2019-11-07 00:0...	11:00:06	1	2/4	00:00:06	38.448	0	0
2019-11-07 00:0...	11:00:07	1	2/4	00:00:07	38.296	0	0
2019-11-07 00:0...	11:00:08	1	2/4	00:00:08	38.448	0	0
2019-11-07 00:0...	11:00:09	1	2/4	00:00:09	38.282	0	0
2019-11-07 00:0...	11:00:10	1	2/4	00:00:10	38.296	0	0
2019-11-07 00:0...	11:00:11 AM	1	2/4	00:00:11	38.492	0	0
2019-11-07 00:0...	11:00:12	1	2/4	00:00:12	38.448	0	0
2019-11-07 00:0...	11:00:13	1	2/4	00:00:13	38.492	0	0
2019-11-07 00:0...	11:00:14	1	2/4	00:00:14	38.296	0	0

Figure 10.3: The electric load table in SQL server

After importing the data into the SQL server, a table is created for this purpose to address all the measured value from the device at different dates and time with certain timesteps.

For the temperature data collection and irradiance data from data logger and spectrometer, the same procedure had been done for making a database for whole solar panel measurement.

However, for importing data, the procedure of importing was different from the weather station. In this sense, the stored data first saved in an excel file or a csv file. Then the file was imported into the database respectively in order to make a complete database for the solar panel measurement.

## 10.5 Cloud Storage

Cloud storage is a remote and virtualized environment to upload data in order to connect and get data from any different location or computer. The major advantage of this storage is being remote and applicable for all users from different locations. However, developing a cloud storage was beyond skills of the current group members. A database for the solar panel was made with SQL server and collected data into the sorted tables.

# 11 Results

This chapter is about the results of real measurements, software, simulation, weather application, the SQL server, and the cloud.

## 11.1 Solar Panel Data Collection

In the following examples of real data tables and the parameters required to calculate heat transfer coefficients are sorted. Some of these data are used to simulate real conditions and compare the results with real data.

### 11.1.1 Electronic Load Data

As described in chapter 9, four tests with different patterns were run. The pattern test 1 gave a number for power and current for a moment, but it was not steady. Other times nothing was shown in pattern test 1 except voltage. Pattern test 2 and 3 did not show power and current, the only number with these sequences was voltage value.

Finally, step 4 which was constant current, showed the power, current, and voltage. The electrical data from sequence 4 (constant current 0.1 A) of test 4 were recorded and sorted in Table 11.1. The accuracy of the device is 3 decimals for numbers.

Table 11.1: The results of pattern test 4 constant current sequence with power measurement.

Date (2019)	Time	Channel	Step	Run Time (s)	Voltage value (V)	Current value (A)	Power (W)
07.11.19	11:00:31	01	4/4	0:00:31	38.240	0.1	3.831
07.11.19	11:00:32	01	4/4	0:00:32	38.042	0.1	3.804
07.11.19	11:00:33	01	4/4	0:00:33	38.052	0.1	3.805
07.11.19	11:00:35	01	4/4	0:00:34	38.056	0.1	3.806
07.11.19	11:00:36	01	4/4	0:00:35	38.052	0.1	3.805

The saving options and exporting options did not work for windows 10 settings. It was attempted to sink the software with windows 10 to make it capable to export data, but it was not successful. The analysis part of the software did not work in windows 10. It was possible to export files as an excel file or notepad, but the numbers were not shown completely. Most of the numbers were zero in the exported file, so the data were recorded manually and saved in excel, then exported to the SQL server.

For the weather condition on 4. November 2019, shading was tested with covering half of the panel with a scarf and running pattern test 4. The result was dropping power generation to 1 W and voltage drop of 14 V.

### 11.1.2 Temperatures measured by the Data Logger

On Thursday 7. November 2019, the solar panel and its equipment were tested outside of the process hall at USN. To measure the temperatures around the solar panel the data logger was used. The sensors to measure the temperature of the panel, both front and back, were attached to the panel with tape. The sensor for the ground was jammed in the ground and the sensor for the air was held over the panel by one of the students. The program was first set to a measured interval of 1 sec, but this was later changed to 30 sec. A selection of the data is shown in Table 11.2. More of the measured data is in Appendix C.

Table 11.2: Some of the measured values from the test 07.11

Date	Time	Temperature Air (°C)	Temperature Panel, Front (°C)	Temperature Panel, Back (°C)	Temperature Ground (°C)
07.11.19	11:45:20	1.0	3.15	2.21	1.1
07.11.19	11:45:50	1.2	3.18	2.23	1.0
07.11.19	11:46:20	1.2	3.21	2.27	1.1
07.11.19	11:46:50	1.2	3.18	2.34	1.2
07.11.19	11:47:20	1.1	3.14	2.25	1.2
07.11.19	11:47:50	1.2	3.23	2.32	1.1

### 11.1.3 Data Collection with the Spectrometer and Weather Station

The measurement of irradiation of the sun was made on November 14. The weather was cloudy and the temperature was around 2 °C. The spectrometer was set up in the window on the second floor so the connection to the computer was possible.

Figure 11.1 shows the raw data of wavelength measured by the spectrometer. The range of the wavelength was approximately 310-1050 nm. On the Y-axis SpectraWiz shows the amount of counts or photons at the specific wavelength. This shows the intensity of the sunlight. The amount of photons is significantly higher for 500-700 nm.

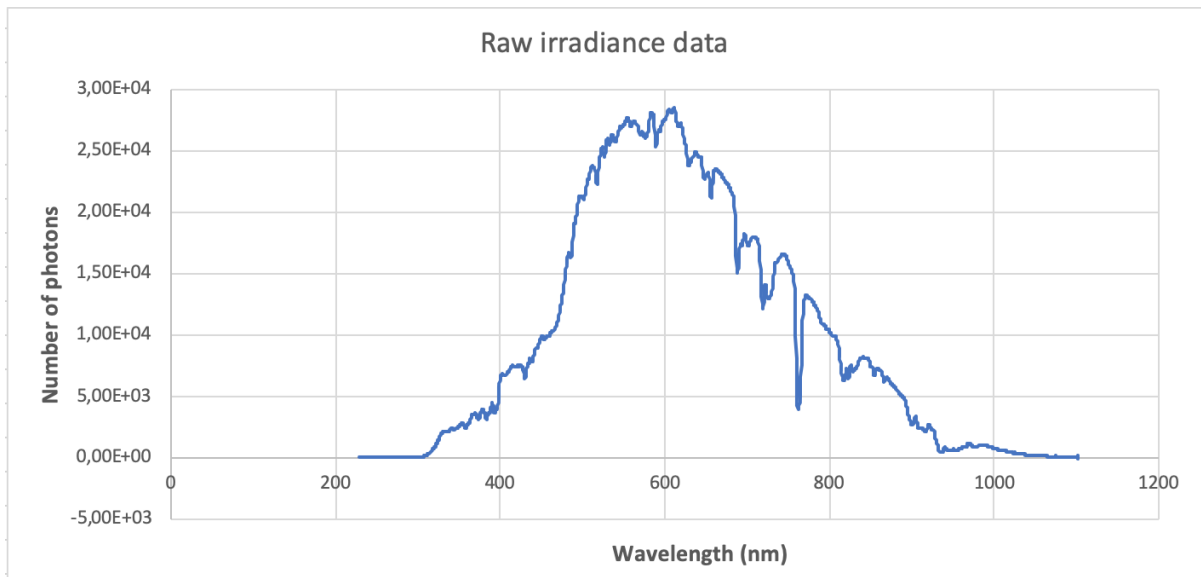


Figure 11.1 Raw data of irradiance measurement on a cloudy day

The measurement was then made for  $\text{W}/\text{m}^2$ . Figure 11.2 shows that the peak of watts is at approximately 450 nm and then decreases towards 920 nm.

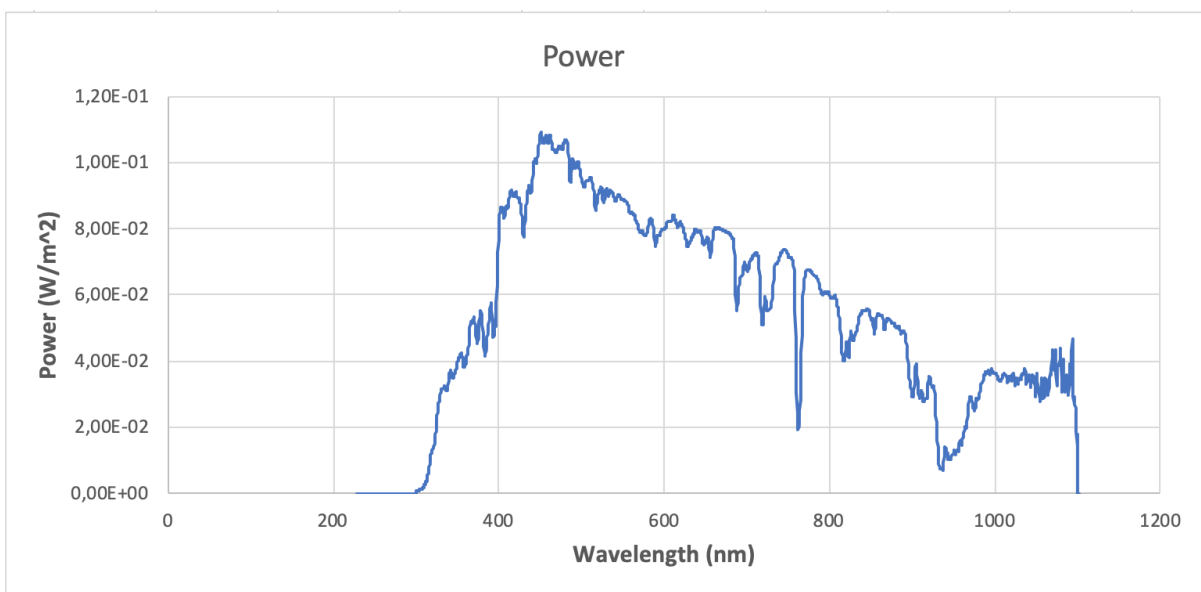


Figure 11.2  $\text{W}/\text{m}^2$  measurement from the spectrometer on a cloudy day

## 11.2 Weather Station

The weather station system from the MicroServer has various parameters. Among all, one is solar irradiation. On the date when the recording data were done, the measured value of solar irradiation from the weather station was approximately  $0.1 \text{ W}/\text{m}^2$ . In this sense, it could be possible to convert the unjustified raw data from the LabView application to check with the value of the real-time engine. However, the difficulty to find the given address from the input registry was demanding and needed more trial to find where the allocated number is placed.

Except the solar irradiation, other parameters were stored in the LabView application for the weather station. In the Table 11.3 the stored data in the LabView were compared with the parameters measured.

Table 11.3: The comparison of the parameters measured from the LabView application and the real-time values at a certain time

Parameters	Date and Time	LabView Measurements	Real Values	Difference in percentage
Temperature( $^{\circ}\text{C}$ )	14/11/2019 18:16:00	3.1	3.1	0%
Humidity(%)	14/11/2019 18:16:00	83%	82%	1.22%
Wind Speed(m/s)	14/11/2019 18:16:00	1.8	1.8	0
Wind Direction( $^{\circ}$ )	14/11/2019 18:16:00	321	287	11.85%
Barometric Pressure(hpa)	14/11/2019 18:16:00	1009	1009	0

As it is shown in Table 11.3, temperature, wind speed and the barometric pressure have no difference from the real values and difference for the humidity from the application and the real value is not significant. However, for the wind direction, the difference shows 11.85%. This significant difference results from change of wind direction every second and the moment the value was measured via LabView was different from the time that was taken from the real value.

### 11.3 Calculations

Based on the heat balance theory of the solar panel, the required parameters for heat balance simulation are calculated. The calculated parameters are gathered in Table 11.4 for the front and the back of the panel. Temperature and irradiance data are based on real data collected from the data logger and spectrometer. The calculations are done based on:

- Air temperature =  $1.1^{\circ}\text{C}$
- Ground temperature =  $1.2^{\circ}\text{C}$
- $G$  for partly cloudy weather on that day was  $28\text{ W/m}^2$ . From the weather station. (For a rainy day in November, the solar irradiation from the weather station was  $0\text{ W/m}^2$ )

Table 11.4: Calculated parameters from reference tables and formula required for simulation.

Parameter	Front surface	Back surface	Obtained by
Temperature	3.14 °C	2.25 °C	Data logger
Film temperature	275.12 K	274.67 K	Averaging based on equation
Wind speed	1.3- 1.8 (m/s)	1.3-1.8 (m/s)	Weather station
Normal Irradiation	50-150	-	Weather station
Angle of panel	45 °	45 °	Mounting
Irradiation to panel	20 W/m <sup>2</sup>	-	By equation
$Pr$	0.713	0.713	Interpolation the data in reference book [29]
K (Thermal conductivity)	0.024 (W/mK)	0.024 (W/mK)	Interpolation the data in reference book [29]
$\nu$	$13.675 \times 10^{-6}$ (m <sup>2</sup> /s)	$13.586 \times 10^{-6}$ (m <sup>2</sup> /s)	Interpolation the data in reference book [29]
$L_c$	0.309 m	0.309 m	Area/perimeter
$Re$	$3.5 \times 10^4 < 5 \times 10^5$ (laminar)	$3.5 \times 10^4 < 5 \times 10^5$ (laminar)	By equation (5.33)
$Gr$	11463352.79	6557849.313	By equation (5.31)
$Gr/Re^2$	$\ll 1$ (Forced convection)	$\ll 1$ (Forced convection)	-
$Nu_{L,forced}$	111.001	111.007	By equation (5.35)
$\bar{h}_{conv}$	8.732	8.704	By equation (5.29)
$F_{ij}$	0.617	0.617	By equation (5.19)
$h_{rad}$	$3.119 \times 10^{-8}$ (W/(m <sup>2</sup> k <sup>4</sup> ))	$2.874 \times 10^{-8}$ (W/(m <sup>2</sup> k <sup>4</sup> ))	By equation (5.18)

For the selected real condition, the airflow around the panel is recognized as laminar flow. Based on the ratio between Reynolds and Grashof number, the convection is obtained as forced convection, so the formula for calculating the Nusselt number is picked based on this information. In that formula, the laminar condition is considered all over the region.

## 11.4 Simulation Results

The result of the simulation is given for STC conditions based on the datasheet, to indicate that the simulation outputs are correct. Then another run is done for real conditions on 7. November 2019.

### 11.4.1 I-V, P-V Curves

Figure 11.3 shows the result of the power simulation. As can be seen, the blue curve is for 25 °C and 1000 W sun irradiation with horizontal placement. The X and Y in the P-V curve are (32 V, 295.1 W) which are very close to the voltage corresponding to the maximum power in the solar panel datasheet. The corresponding current is very close to the amount in the datasheet, which is (32.03 V, 9.21 A) at maximum power: 295 W. The error of power simulation is 0.03 % which very close to zero.

In order to have more certainty about the simulation accuracy, two temperatures 35 °C and 45 °C is tried. The power obtained for these temperatures is lower than that in STC conditions.

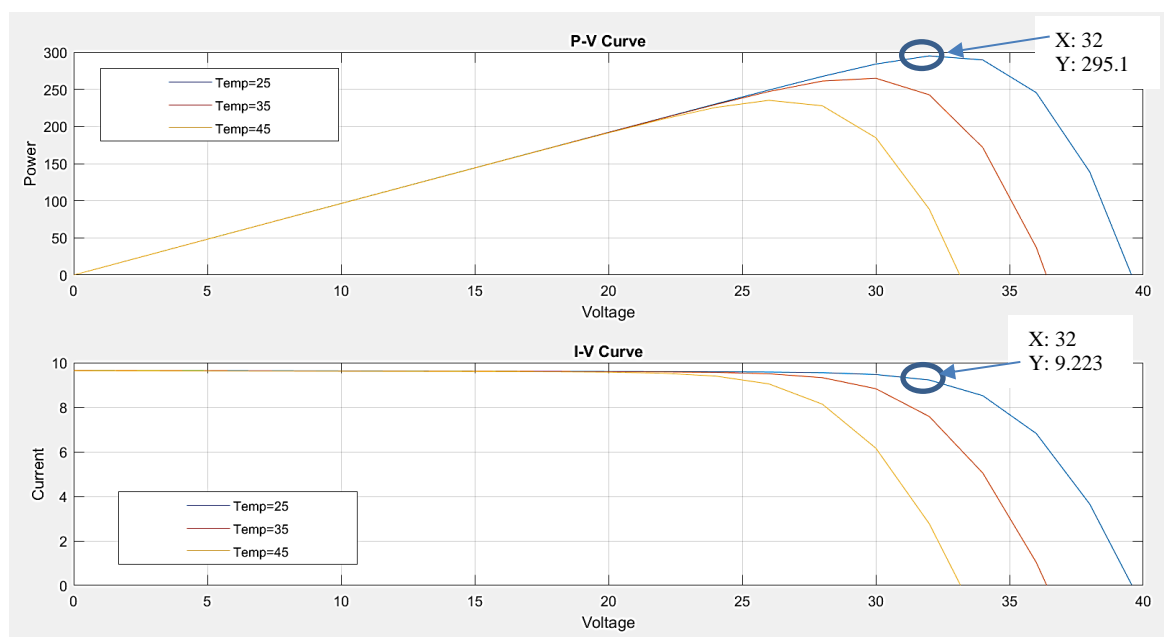


Figure 11.3: P-V, I-V curves by simulation for 25, 35 and 45 °C and 1000 W/m<sup>2</sup> irradiation.

Simulation for real conditions is done for the temperature -2 °C and the solar irradiation of 28 W/m<sup>2</sup>. The amount of solar irradiation is obtained from the weather station and the effect of angle is involved.

As can be seen in Figure 11.4, in the mentioned conditions, the maximum power for the blue line in the P-V curve which corresponds to -2 °C occurs in the point (38 V, 3.387 W). Also, in the I-V curve, the corresponding current at the point 32 and 38 V can be seen in the figure.



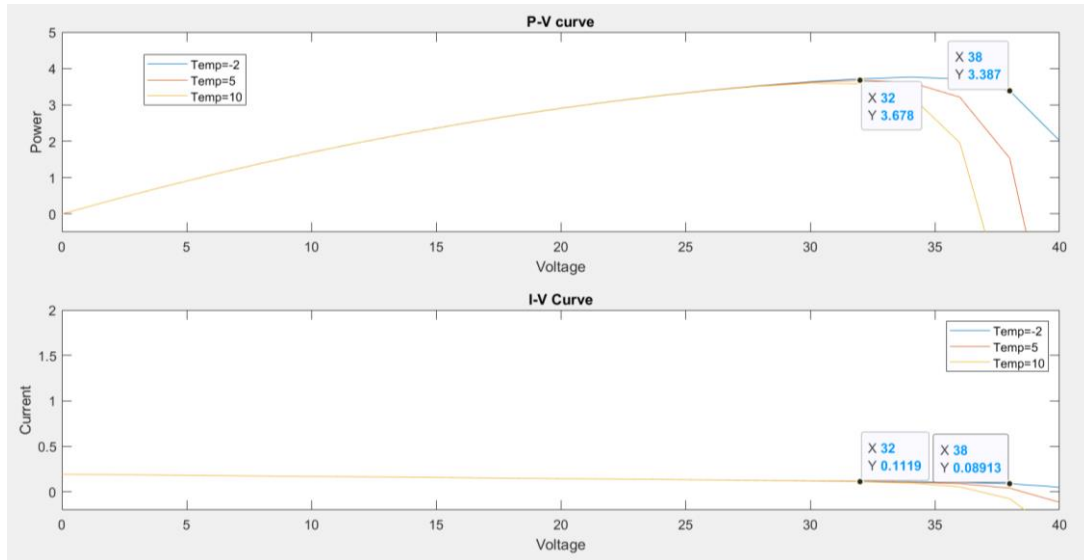


Figure 11.4: Simulation results of power generation for -2, 5, 10 °C with 28 W/m<sup>2</sup> irradiation.

### 11.4.2 Heat Balance Simulation

Results of heat balance are obtained for two conditions as is described as following. Temperatures of each contact surface for all layers are obtained after inserting calculated heat transfer parameters in the simulation for -2 °C and 20 W/m<sup>2</sup> irradiation.

The open-circuit simulation is done for the same values considering all the 3.387 W power is wasted as heat.

As the outdoor measurement data are for a minus zero weather, they do not give different values to see how the temperatures change in different layers. Thus, the simulation is run for 25 °C and 1000 W/m<sup>2</sup> of irradiation with relevant heat transfer coefficients.

Running the simulation for 25 °C and 1000 W/m<sup>2</sup> of irradiation in open circuit conditions gives 295 W additional energy as heat. The simulation results for the open and closed-circuit for both conditions are sorted in Table 11.5.

Table 11.5: Results of layer temperatures for different temperatures and irradiation values in close and open circuit.

The temperature of the Layer	Temperature of the Contact Surface (K) for -2 °C and 20 W/m <sup>2</sup> of irradiation (Experimental)		Temperature of the Contact Surface (K) for 25 °C and 1000 W/m <sup>2</sup> irradiation (STC)	
	Closed-circuit	Open-circuit	Closed-circuit	Open-circuit
$T_s$ (Input)	276.14	276.14	303	303
$T_g$	276	276.1	311.6	311.8
$T_{eva,1}$	276	276.1	311.9	312.1
$T_{si}$	276	276.1	311.9	312.1
$T_{eva2}$	275.9	276	310.9	311
$T_{pvf}$	275.9	276	310	310.1
$T_b$ (Input)	275.25	275.25	301	301

### 11.4.3 DC/AC Simulation

The resulted graphs from the DC/AC simulation can be seen in Figure 11.5: and Figure 11.6.

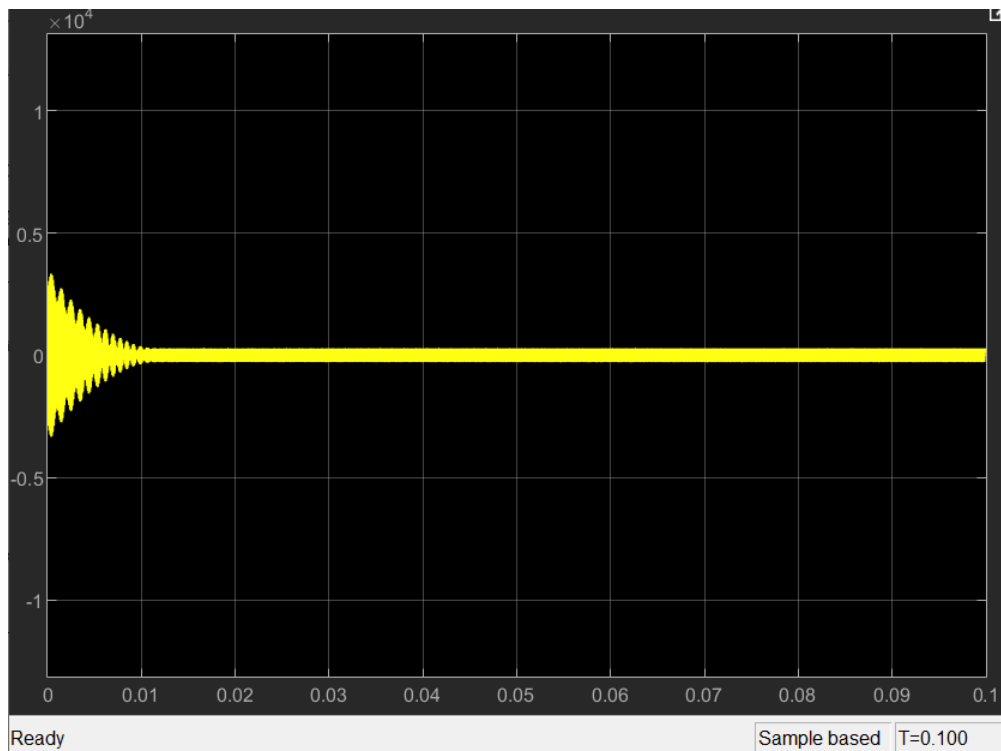


Figure 11.5: Total shape of the sine wave until 0.1 s.

Every 12 DC voltage, converts to 220 V of AC voltage. So, for 30.2 V of DC source, the amplitude is between -400 and +400 V of AC current.

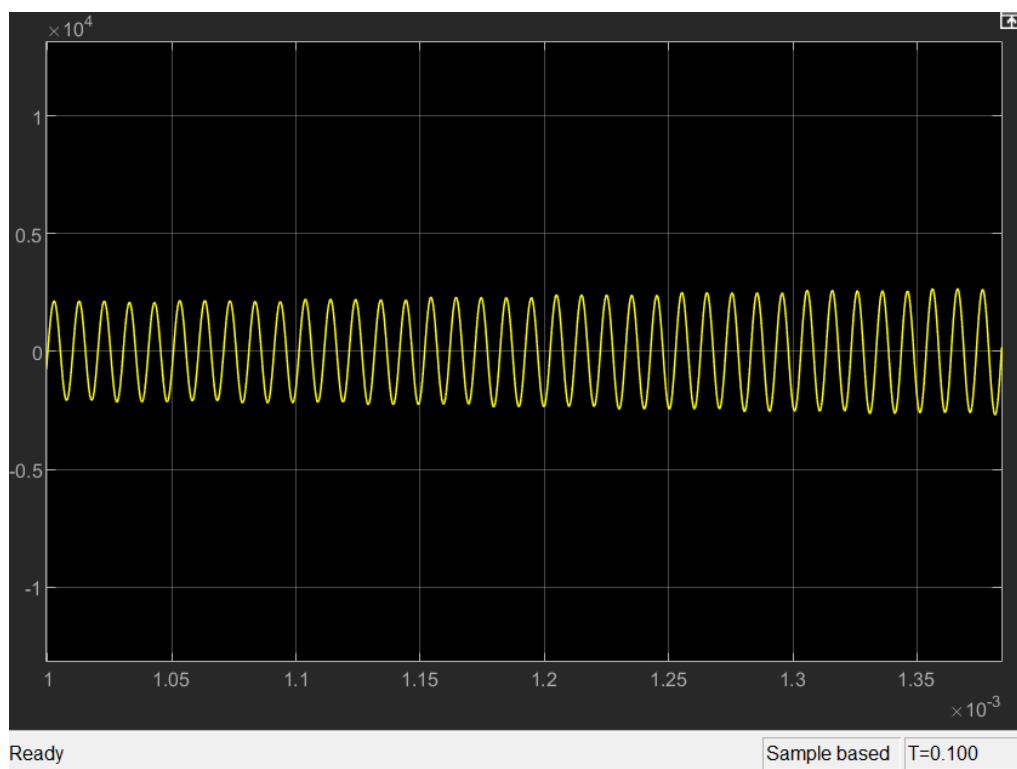


Figure 11.6: DC/AC conversion result with zoom-in.

# 12 Discussion

The results of the project are discussed in detail in this chapter.

## 12.1 Solar Panel outdoor measurements

The purpose of data collection from solar panels is to find out which days in the year or in a season provide more electrical power. Another considerable factor is the angle of the solar panel with the sun. This is important in order to investigate the proper angle to absorb more solar energy during the day or the week.

As another consideration, cooling the solar panel is important for the optimum functionality. Thus, the location should provide all these items to obtain more power generation from the solar panel.

According to these terms, the solar panel should be on the roof of a building or in a wide area where the surrounding is open and no shadow covers the panel. In addition, the ventilation around the panel should be provided by surrounding air for cooling aspects.

No appropriate placement to collect valuable measurement data was provided until the end of the project. In addition, measurements could not be done on rainy or snowy days as it was not possible to keep electric devices in that condition without a waterproof cover.

According to weather station data, the irradiation was zero for most of the days. So, continuous data collection was not worthy. The flat area outside the process hall of B building at the USN, which was surrounded by other buildings, was not a convenient place for outdoor measurement.

However, it was the only possible place to have access to electric plugs. So, the outdoor measurement was carried out in order to have real data for the power generation and heat balance simulation. Although the power generation is very low during the cloudy days with minus zero temperature, there are still a few watts of power generation.

Shade acts as an insulator and prohibits the light absorption to the panel so it reduces the power generation.

### 12.1.1 Electric Data

After getting familiar with LinkView, the sequence that shows the power amount was found to be the constant current mode with the value of 100 mA as shown in Figure 9.4. The test was repeated and the electric data were the same. So, the appropriate set up to have power measurement is on constant current.

Long cables connected to the solar panel have higher potential resistance and inductance. In order to compensate for induction, the solar panel connection wires can be twisted.

It was found that the sequences can be saved in internal memory or USB but no procedure was found to save data except LinkView and Realterm.

The attempt for saving data in LinkView was only Excel files with some setting values for testing patterns and many columns with zero values. Hence it seems that the GWINSTEK version does not sink with Windows versions higher than Windows 8. Likewise, the attempt for capturing data with Realterm that was recommended in the instruction was not successful.

As the serial port monitor program needs interpretation of computer science, it was found that only zeros with two different data length mean that the connection is on and off. But no data were captured. Two programs cannot get valuable data from the same device so it is probably

due to the version of the device which is not capable of saving data. Likewise, writing a program to capture data was not possible because the full information about the device and its microcontrollers was not possible to retain for this project.

Thus, the data were recorded manually for this electronic load. Furthermore, it was found that this device does not have the capability to be controlled by LabView as it lacks the connection port.

### 12.1.2 Temperature Data

Automatic download of the measured temperatures needed Squirrelview plus software and the license was not available during the project. Therefore, manually download was used in this project. The temperature measured was at steady state, so the values are assumed to be credible.

When setting up the data logger, the bachelor report was used as a guideline. Turns out they used to type of sensors, PT1000 and Thermocouple. In this project, only PT1000 sensors were used. Therefore, the setup used when testing the solar panel were wrong. A test was performed inside to check the difference in measured temperatures with different setup. This showed some difference, the thermocouple measured temperatures about 1°C lower than the PT1000 sensor. This is shown in appendix D. This was discovered very late in the project and new measurements outdoors were not possible.

### 12.1.3 Irradiance Data

The irradiance data was collected on a different day than the other outdoor measurements. The weather conditions were approximately the same, but some variations in clouds at the exact measurement may have caused different data. The spectrometer sensor was set in the window of the second floor above the solar panel standing outside. This difference in height and angle may result in other irradiance conditions for the spectrometer and the solar panel. When comparing the measurements in Figure 11.2 with the reference ASTM curve in Figure 8.5 there are similarities between the curves. The ASTM curve has a higher maximum point than the measured data, but the outlines of the curves are approximately the same. Both curves increase towards 500 nm and has a drop at approximately 750 and 1100 nm. Considering this comparison of this data only, the measurements from the spectrometer are correct but not accurate enough to draw a conclusion. The acquire accurate data, several measurements in different weather conditions is required.

The measured data is also based on a manual dark baseline. This baseline will not be completely accurate considering an object was manually placed over the sensor. The object may be placed differently for each measurement causing small variations. As mentioned in chapter 8 an automatic baseline and automatic data collection would optimize the accuracy of the results.

### 12.1.4 Weather station

In this project, the ModBus protocol had been used to make the connection between the server and the client. This protocol used a Master/Slave structure where the server acts as a slave to wait for the request and make the connection to sensors and the client has the role of maser to request reading data to the slave. After developing the application in the LabView with the given IP address to collect data from the weather station, the program will read different values. With the equation (7.1), all data are converted from raw unjustified 16-bit integers to real values. However, finding the exact parameters correspond to their real value needs a significant number of tries. In this project, the major important parameters such as temperature, humidity,

wind speed, wind direction and barometric pressure. After converting data, it was found that the application shows the same values as the real value.

In addition, in this project it was asked to make cloud storage for this case. After a time, it was found that developing a cloud database solely for this project, needs more time and knowledge background about the Information Technology, which unfortunately none of the group members had the relevant background.

## 12.2 Simulation

This section is discussion the results of power, heat and DC/AC inverter simulation.

### 12.2.1 Power Generation Simulation

The power generation model is completely in agreement with the values in the datasheet for STC conditions. As can be seen in Figure 11.3, the simulation for P-V and I-V curves fit with the maximum power point. The corresponding voltage to maximum power was at the point (32 V, 295.1 W) that is very close to real data (32.03 V, 295 W). Comparing the current values, the simulation point is (32 V, 0.922 A) at maximum power while the real data are (32.03 V, 9.21 A).

The error of power prediction can be calculated as 0.03 % for STC conditions. Thus, the simulation results are valid and reliable. This means all the assumptions taken for simulation are correct and the circuit of the solar panel is a single-diode circuit with shunt and series resistor.

Another prediction that is carried out by the simulation is power generation in different temperatures or different amounts of solar irradiation. For example, it is obvious in the figure that in the same amount of solar irradiation, less power is generated in higher temperatures. When a simulation program is available, it is very easy to predict different conditions of temperature, irradiation and the angle of the solar panel.

Evaluating the simulation with real data can be seen in Figure 11.4. As it is clear, the simulation figure shows the point (38 V, 3.387 W) for the P-V curve and (38 V, 0.0891 A) for I-V curve. In Table 11.1, the average of real measurements is about 38.1 V and the average power is about 3.8 W. So, the error is 3.8 % that is an acceptable amount. The reason that the error of the simulation becomes higher compared to STC condition values is because of the power loss across the cables and resistors in the electronic load.

As the error is acceptable, it can result in that the constant current is the correct mode for running the electronic load.

Also, the figure shows that the higher temperature results in lower power generation at the same irradiation which is in accordance with practical measurements that have been done in the bachelor project.

### 12.2.2 Heat Simulation

The results of heat simulation are sorted in Table 11.5. As it is seen, for closed-circuit conditions at  $-2^{\circ}\text{C}$  and  $20\text{ W/m}^2$  of irradiation, the temperature profile from the front surface to the back of the panel is a decreasing profile. Due to the ambient temperature and a few watts of power generated, the layers do not show a considerable difference in temperature. But it is obvious that the silicon layer has a higher temperature than the two bottom layers of the solar panel.

It is meaningful because the short wavelengths cause heating the two layers above the silicon layer and long wavelengths cause heating the two bottom layers if they pass the silicon layer, but some of that may be reflected. Those long waves which are reflected by the silicon layer cause more heat to upper layers. Therefore, it is expected to have higher temperatures at the upper layers.

The reflected infrared and the prohibited ultraviolet arrays cause the first and second top layers generating more heat, so the temperature is higher at the two top layers. The temperature of the glass is lower than EVA1 due to the convection by Newton's cooling law. At the bottom, lower heat is absorbed by the two bottom layers. That causes less temperature compared to the top three layers. The PVF layer is cooler because of convection at the back surface.

In open-circuit, the silicon layer is stimulated, and the electron transfer occurs during the irradiation. If there is no current flow, the layers of the silicon wafer become saturated. This makes the silicon layer willing to reach a steady state. So, the power will be dissipated as heat.

The effect of open-circuit voltage when there is no load causes heating the solar panel and the existence of a shunt resistor makes the panel be safe and not damaged if the power uptake (load) is off. It forbids the power leakage. The electric potential will be lost in the form of heat causing an increase in the silicon layer temperature and maybe an increase in other layers as well.

As can be seen, adding heat causes an increase in layer temperatures. Also, the higher amount of power loss as heat, makes a little higher increase in layer temperature. The temperature of the silicon layer is the same as the EVA1 layer. It might be due to the thickness of the silicon layer which is only 18 microns.

### 12.2.3 DC/AC inverter

There was no real inverter in the project so as a simple DC/AC simulation, the sine wave plot is shown in Figure 11.5: for some assumption values for time delay, amplitude, and resistors. The oscillation and dissipation of the sine wave occur smoothly until 0.01 s. As the figure shows, the values which were picked from examples in the Simulink tutorial are in good agreement with converting 12 volts of DC electric source to 220 volts of an AC electric source.

# 13 Conclusion

This project was carried out on:

- Mounting the solar panel on the roof in order to collect continuous outdoor data
- Measure the power generation by the time and examine the effect of weather conditions on power generation
- Simulation the power generation plus DC/AC inverter and heat balance
- Automate data collection and making a cloud storage
- Develop a weather data saving application and export to a cloud storage

Setting up devices and software was done successfully in order to examine the power generation with outdoor measurements. The constant current mode for the electronic load showed the power amount.

Since the solar panel had no fixed place until the end of the project, the continuous data collection by time has become in the future work frame. So, the outdoor measurements ended up providing real data in order to validate the simulation task.

The simulation of power generation was performed based on the single-diode model with resistors. The simulation had high accuracy comparing the simulation outputs with real power measurements. The observation of real data and simulation confirmed that at constant sun irradiation, the power generation increases with the decrease in weather temperature. In addition, a few watts of power can be generated in minus zero degrees in partly cloudy days in the autumn.

The heat balance simulation in order to predict the panel layer temperatures was carried out using real data. The outputs were in the range of the surface and back temperatures. In addition, an increase in layer temperatures in open-circuit as the power is lost to heat was observed in the simulation.

Since there was no connection to the electricity grid in order to have real DC/AC data, a DC/AC inverter was simulated only to observe true sin wave oscillation and dissipation of voltage graphs.

In order to automate data collection, the procedure of temperature data saving in a cloud was found. It can be purchased and implemented. No procedure was found for automatic data saving for the electronic load because of the compatibility of its version with serial data capturing software, so power data was recorded manually.

One spectral irradiance measurement was accomplished with the spectrometer. With only one data sample, there cannot be made a correct conclusion. For the spectral data manipulation, a Lab View program is available, but it cannot save spectral data automatically. The limitations to have all required software on one computer put this task in the future work frame.

The weather data saving application is developed. It is able to save weather temperature, wind speed, wind direction, and humidity at any time but not continuously. The time of the project and more knowledge in IT technology put further work on automatic continuous data saving with this application in the future work frame.

As the final task a database was developed for both weather station data and solar panel measurements. All stored data were collected into the right database.



## 14 Further Work

The task description consisted of many parts, where some tasks were impossible to accomplish during this group project. Several tasks were completely related to IT, software technology and maybe mechatronic and electrical power engineering. Further work on this project can be done in these areas:

For spectral data, a dark spectrum baseline correction is needed. A mechanism for this should be constructed. This means that a mechanical object that is controlled by a controlling program should be constructed to provide the baseline automatically as the spectrometer starts measurement. Automatic data collection from the spectrometer is also needed.

Practical work is required for DC/AC conversion with real inverter and connection to the utility grid to apply controller on the power generation.

A good placement should be provided for the solar panel and its accompanying devices to be able to get valuable power data and observing shading effects.

In order to automatize data collection, it is better to provide newer measuring devices that have the ability in their features.

# References

- [1] S. J. Fonash, R. T. Fonash, and S. Ashok, "Solar cell," in *Solar Cell*, ed. Britannia.com: Britannia.com, 2017.
- [2] K. Hofstad, "Solenergi," in *Store Norske Leksikon*, ed, 2019.
- [3] S. Ashok, "Solar Energy," in *Britannia.com*, ed. Britannia.com, 2018.
- [4] T. E. o. E. Britannica, "Photovoltaic effect," in *Britannia.com*, ed. Britannia.com, 2006.
- [5] S. A. Kalogirou, *Solar Energy Engineering*, 1. ed. Academic Press, 2009.
- [6] A. Blakers, "Explainer: what is photovoltaic solar energy?," 26.03.2013. [Online]. Available: <https://theconversation.com/explainer-what-is-photovoltaic-solar-energy-12924>
- [7] E. J. Øverlid, "How well do solar cells really work in the Nordic climate?," 16.03.2018. [Online]. Available: <https://www.sintef.no/en/latest-news/how-well-do-solar-cells-really-work-in-the-nordic-climate/>
- [8] O. Hølland, "Renewable: First floating solar power plant." [Online]. Available: <https://explained.statkraft.com/articles/2019/renewable-first-floating-solar-power-plant/>
- [9] Ocean Sun. "Solutions." Ocean sun. <https://oceansun.no/products/> (accessed 02.10.19, 2019).
- [10] The Explorer. "Pioneering floating solar power solutions." The Explorer. <https://www.theexplorer.no/solutions/ocean-sun--pioneering-floating-solar-power-solutions/> (accessed 02.10.19, 2019).
- [11] Multiconsult, "Starting innovative research on hybridization of hydropower with floating solar," 29.03.19. [Online]. Available: <https://www.multiconsultgroup.com/starting-innovative-research-on-hybridization-of-hydropower-with-floating-solar/>
- [12] S. Forsdick, "How floating solar panels could make make hydroelectric power more reliable," 01.04.19. [Online]. Available: <https://live-newstatesman-b2b.pantheonsite.io/floating-solar-panels/>
- [13] K. E. S. M. H. A. O. J. O. S. A. S. V. Romaikin, "Design, bygging og testing av testtrigg for alternative plasseringer av solcellepaneler," Bachelor, Fakultet for teknologi, naturvitenskap og maritime fag, Universitetet i Sørøst-Norge, Universitetet i Sørøst-Norge, 2019.
- [14] Ecodirect. "JA Solar JA-JAM60-S02-295PR-BK > 295 Watt Mono Solar Panel - BoB." <https://www.ecodirect.com/JA-Solar-JA-JAM60-S02-295PR-BK-295W-Solar-Panel-p/ja-solar-ja-jam60-s02-295pr-bk.htm> (accessed 09.11, 2019).
- [15] Grant Instruments. "SQ2020." <https://www.grantinstruments.com/data-acquisition/squirrel-loggers/sq2020> (accessed 15.10, 2019).
- [16] Farnell. "PEL-3031E - DC Electronic Load, PEL-3000E Series, 300 W, Programmable, 1 V, 150 V, 60 A." <https://no.farnell.com/gw-instek/pel-3031e/dc-electronic-load-1-channel-150v/dp/2930376> (accessed 09.11, 2019).
- [17] PlusPNG. "Computer HD PNG-PlusPNG." <http://pluspng.com/png-93319.html> (accessed 09.11, 2019).
- [18] StellarNet. "BLACK-Comet UV-VIS Spectrometer." <https://www.stellarnet.us/spectrometers/black-comet-uv-vis-concave-grating-spectrometers/> (accessed 09.11, 2019).
- [19] PERCIUM 285-305 1000V Black Module Series, 285-305/PR. [Online]. Available: <https://solarnrg.nl/downloads/product-sheets/product-sheet-ja-solar-jam60s02-295-pr.pdf>.

- [20] Sino Voltaics. "Normal Operating Cell Temperature (NOCT): definition." <https://sinovoltaics.com/learning-center/quality/normal-operating-cell-temperature-noct-definition-noct-definition/> (accessed 20.10, 2019).
- [21] *DC Electronic load PEL-3000E User Manual*, GWINSTEK, 1.11. [Online]. Available: <https://www.gwinstek.com/en-global/products/detail/PEL-3000E>.
- [22] GW Instek. "PEL-3000E." <https://www.gwinstek.com/en-global/products/detail/PEL-3000E> (accessed 10.10, 2019).
- [23] *Squirrel 2020 Series*. Accessed: 15.10.2019.
- [24] Pico Technology. "PT100 platinum resistance thermometers." <https://www.picotech.com/library/application-note/pt100-platinum-resistance-thermometers> (accessed 15.10, 2019).
- [25] BWTEK. "How does a spectrometer work?" BWTEK. <https://bwtek.com/spectrometer-introduction/> (accessed 13.10.19, 2019).
- [26] StellarNet Inc. "BLACK-Comet-SR Spectrometer." StellarNet Inc. <https://www.stellarnet.us/spectrometers/black-comet-sr/> (accessed 13.10.19, 2019).
- [27] National Instruments. "What Is Data Acquisition?" <http://www.ni.com/data-acquisition/what-is/> (accessed 02.11, 2019).
- [28] M. Rouse. "cloud database." <https://searchcloudcomputing.techtarget.com/definition/cloud-database> (accessed 02.11, 2019).
- [29] T. L. Bergman, F. P. Incropera, D. P. DeWitt, and A. S. Lavine, *Fundamentals of heat and mass transfer*. John Wiley & Sons, 2011.
- [30] Weather Spark. "Average Weather in Porsgrunn." <https://weatherspark.com/y/65492/Average-Weather-in-Porsgrunn-Norway-Year-Round> (accessed 04.11, 2019).
- [31] S. Irvine, "Solar Cells and Photovoltaics," in *Springer Handbook of Electronic and Photonic Materials*, S. Kasap and P. Capper Eds. Cham: Springer International Publishing, 2017, pp. 1-1.
- [32] M. N. I. Sarkar, "Effect of various model parameters on solar photovoltaic cell simulation: a SPICE analysis," *Renewables: Wind, Water, and Solar*, journal article vol. 3, no. 1, p. 13, August 12 2016, doi: 10.1186/s40807-016-0035-3.
- [33] M. Hammami, S. Torretti, F. Grimaccia, and G. Grandi, "Thermal and performance analysis of a photovoltaic module with an integrated energy storage system," *Applied Sciences*, vol. 7, no. 11, p. 1107, 2017.
- [34] All About Circuits. "Introduction to Diodes And Rectifiers." <https://www.allaboutcircuits.com/textbook/semiconductors/chpt-3/introduction-to-diodes-and-rectifiers/> (accessed 11.10, 2019).
- [35] M. Seifi, A. che soh, N. Izzrib.Abd.Wahab, and M. K. Hassan, *A Comparative Study of PV Models in Matlab/Simulink*. 2013.
- [36] K. Pickerel. "The PV junction box: An overlooked, yet important part of a polar panel " <https://www.solarpowerworldonline.com/2017/05/pv-junction-box-overlooked-yet-important-part-solar-panel/> (accessed 03.11, 2019).
- [37] PV Education. "Equations for Photovoltaics." <https://www.pveducation.org/pvcdrom/appendices/equations/equations-for-photovoltaics> (accessed 11.10, 2019).
- [38] PV Education. "Fill Factor." <https://www.pveducation.org/pvcdrom/solar-cell-operation/fill-factor> (accessed 15.10, 2019).
- [39] T. Haumann, T. Bostr?m, and M. Berner, "A Brief Look at the Performance of PV in Norway," ed: UiT The Arctic University of Norway, 2016.

- [40] Energy Matters. "Grid connected solar panel systems." <https://www.energymatters.com.au/grid-connected-solar/> (accessed 03.11, 2019).
- [41] Energy Matters. "Solar inverters: Micro, String and Central." <https://www.energymatters.com.au/components/micro-string-central-inverters/> (accessed 03.11, 2019).
- [42] Energy Matters. "A guide to power inverters / solar inverters." <https://www.energymatters.com.au/components/inverters/#Sinewaveinverters> (accessed 03.11, 2019).
- [43] ThermoWorks. "Infrared Emissivity Table." <https://www.thermoworks.com/emissivity-table> (accessed 20.10, 2019).
- [44] MathWorks. "Simscape." <https://www.mathworks.com/products/simscape.html> (accessed 10.10, 2019).
- [45] MathWorks. "Thermal models." <https://www.mathworks.com/help/phymod/simscape/thermal-models.html> (accessed 10.10, 2019).
- [46] *Weather MicroServer User Manual*, 2008.
- [47] Pixabay. <https://pixabay.com/vectors/router-wireless-network-connection-157597/> (accessed 01.10, 2019).
- [48] A. Gurhan, "Design and Development of Windows Store Application for Measurements and Monitoring," Master, Faculty of technology, University of Southeastern Norway, 2013.
- [49] *Capricorn 2000EX weatcher Station Brochure*, <https://columbiaweather.com/products/weather-stations/legacy/capricorn-2000ex-weather-station/>, 2011.
- [50] National Instruments. "Introduction to Modbus using LabVIEW." <https://www.ni.com/en-no/innovations/white-papers/12/introduction-to-modbus-using-labview.html> (accessed 10.10, 2019).
- [51] Realterm. "Realterm: Serial Terminal." <https://realterm.sourceforge.io/> (accessed 05.11, 2019).
- [52] Grant Instruments. "SquirrelView & SquirrelView Plus Software." [http://www.electrometers.com/Assets/PDF\\_files/Grant/SquirrelView.pdf?fbclid=IwAR1RJJMmI\\_3zlmSjYMmk1D7GMI-jacbCqaZHKXyQAVvVWe7KZahnbUAsRJI](http://www.electrometers.com/Assets/PDF_files/Grant/SquirrelView.pdf?fbclid=IwAR1RJJMmI_3zlmSjYMmk1D7GMI-jacbCqaZHKXyQAVvVWe7KZahnbUAsRJI) (accessed 20.10.2019).
- [53] StellarNet. "SpectraWiz Spectroscopy Software." <https://www.stellarnet.us/software/> (accessed 20.10, 2019).
- [54] NREL. "Reference Air Mass 1.5 Spectra." NREL. <https://www.nrel.gov/grid/solar-resource/spectra-am1.5.html> (accessed 14.11.19, 2019).
- [55] Datalogger inc. "Setting Automatic Scheduled Downloads Using the Grant Downloader." <https://www.dataloggerinc.com/resource-article/setting-automatic-scheduled-downloads-using-grant-downloader/> (accessed 01.11, 2019).
- [56] Microsoft. "Structured Query Language (SQL)."  
" <https://docs.microsoft.com/en-us/sql/odbc/reference/structured-query-language-sql?redirectedfrom=MSDN&view=sql-server-ver15> (accessed 10.11, 2019).

# Appendices

## Appendix A: Single-diode and Two-diode Model

### A.1: Two-diode Model

When two diodes are used in parallel with lumped and shunt resistors, more accuracy can be achieved because nonlinear P-V curves are simulated. Figure A.1 shows such a circuit. The current superposition is more accurate than single-diode models.

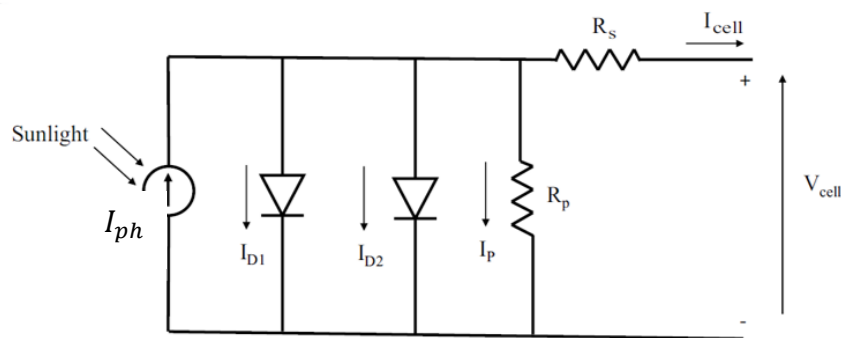


Figure A.1: A scheme of the circuit of the two-diode model.

The cell current equation of a two-diode model is given in equation (A.1).

$$I_{cell} = I_{ph} - I_{01} \left[ \exp \left( \frac{V_{cell} + I_{cell} R_s}{V_{T1}} \right) - 1 \right] - I_{02} \left[ \exp \left( \frac{V_{cell} + I_{cell} R_s}{V_{T2}} \right) - 1 \right] - \frac{(V_{cell} + I_{cell} R_s)}{R_p} \quad (A.1)$$

During the calculation, the ideality factor of the first diode is considered equal to one and for the second diode, it is considered equal to two in most cases.

### A.2: Three-diode Model

Figure A.2 shows the ideal circuit of the three-diode model of PV cell.

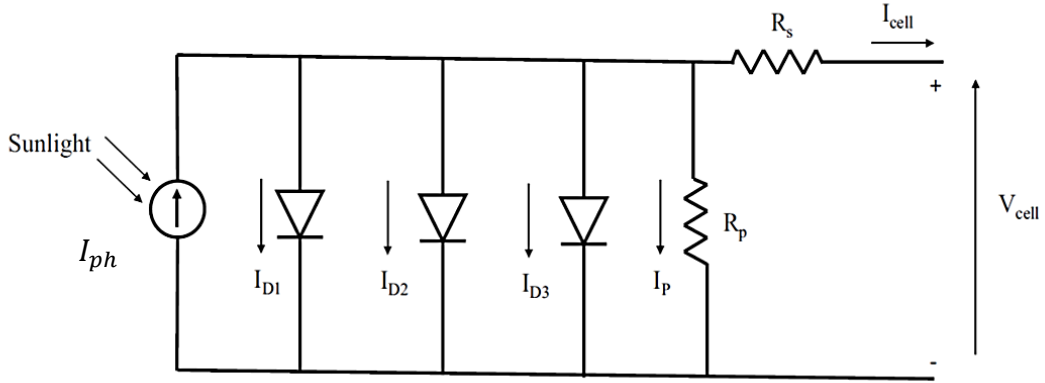


Figure A.2: Ideal three-diode model of PV cell. [32]

The reason of using the third diode in the PV cell circuit is to consider the effect of leakage current through the peripheries and grain boundaries. So, another diode is added to a two-diode model in a parallel configuration. This makes the model complicated, but some parameters are usually ignored during the simulation. The current of the three-diode model is obtained by equation (A.2).

$$I_{cell} = I_{ph} - I_{D1} - I_{D2} - I_{D3} - I_p \quad (\text{A.2})$$

This model is useful to analyse the properties of multi-crystalline silicon PV cells. Inserting the equation corresponding to each parameter leads to equation (A.3). [32]

$$I_{cell} = I_{ph} - I_{01} \left[ \exp \left( \frac{V_{cell} + I_{cell} R_s}{V_{T1}} \right) - 1 \right] - I_{02} \left[ \exp \left( \frac{V_{cell} + I_{cell} R_s}{V_{T2}} \right) - 1 \right] - I_{03} \left[ \exp \left( \frac{V_{cell} + I_{cell} R_s}{V_{T3}} \right) - 1 \right] - \frac{(V_{cell} + I_{cell} R_s)}{R_p} \quad (\text{A.3})$$

Project Task description

## FM4017 Project

**Title:** Solar Panel Data Collection and Heat Balance

**USN supervisor:** Kjell-Arne Solli (PEM), Hans-Peter Halvorsen (EIK)

**External partner (part time):** Proventia, Suncells Scandinavia AS / Jan Bjarne Lid, (Kraggerø Energi or Skagerak Energi)

### **Task background:**

Electric power from solar panels has a high potential for contribution to the global demand for power and low CO<sub>2</sub> emissions. The power generated from photovoltaic (PV) cells is influenced by temperature, irradiation intensity, and sunlight spectral composition. Positioning of solar panels on a lake or ocean can potentially increase power efficiency and reduce conflicts related to the use of the land area.

A bachelor project was accomplished in spring 2019 targeted on modeling the power from one solar panel, as well as the heat balance, based on spectral irradiation and temperature measurements. A test rig and instrumentation was built for this purpose, and some measurements performed outdoor and indoor (artificial light, spectral analysis of irradiation, temperatures, panel power). The solar panel, as well as instruments, were purchased by Proventia, and the project financed by Proventia with partners and Suncells Scandinavia.

Suncells Scandinavia is aimed at commercializing the production of a raft with solar panels for the delocalized production of electric power utilizing water areas. It is planned for building two grid-connected pilot rafts each of 36 panels (on an 11×11 m raft) in a pre-project autumn 2019. The instrumentation might also serve as a site for PV reference solar measurements. Per August 2019, the capital needed for the investments is not yet ready.

### **Task description:**

1. Continue work on solar panel heat balance description and simulation based on outdoor measurements using the test rig. Location for outdoor measurements will be provided at USN campus Porsgrunn by Statsbygg. Optionally add instrumentation for total solar irradiation and wind, eventually shading observations.

2. Automatize data collection. For spectral data, a dark spectrum baseline correction is needed, and a mechanism for this should be constructed. Have data saved to a cloud-based service.
3. Develop a simulation model for PV power generation including heat balance (build upon bachelor work and literature).
4. Contribute to the instrumentation design of solar panel rafts as PV reference solar measurements. This would include a remote operation of spectral measurements, for which an automated aperture control based on task 2 (Agreement from an external partner is required).
5. Perform data measurements and collection from solar panel rafts (if available).
6. Eventually include DC-AC inverter variables and properties into a simulation model for power generation, if possible.

**Project objective:** Develop heat balance simulation of solar panels into a tool for power estimation from solar panel arrays based on local climate, as well as land versus sea placement. Develop automatized data collection for reference solar measurements, panel temperature measurements, and PV array power generation. Potentially demonstrate the data collection.

**Group Members:**

Vafa Ahmadi (PT)

Marrienne F. Heitmann (EET)

Marthe Nergård (PT)

Seyyedarash Zarrinkia (EET)

**Practical arrangements:**

*To be decided*, test rig placement at the USN campus. Placement of the solar panel rafts are tentatively planned near Kragerø harbor, but discussions with Skagerak Energi is ongoing. For potentially some work in Kragerø.



**Signatures:** Students and Supervisors

  
 \_\_\_\_\_ 18.09.2019 Porsgrunn  
 Vafa Ahmadi Dato/Sted

  
 \_\_\_\_\_ 18.09.19. Porsgrunn  
 Marianne F. Heitmann Dato/Sted

  
 \_\_\_\_\_ 18.09.19 Porsgrunn  
 Marthe Nergård Dato/Sted

  
 \_\_\_\_\_ 18,09,19 Porsgrunn  
 Seyyedarash Zarrinkia Dato/Sted

\_\_\_\_\_  
 Kjell-Arne Solli Dato/Sted

\_\_\_\_\_  
 Hans-Petter Halvorsen Dato/Sted

Appendix C: Temperature measured with the Data logger.

Date/Time	Type	tempAir ('C)	tempPanelFront ('C)	tempPanelBack ('C)	tempGround ('C)
07.11.2019 11:38	Interval	1,10	2,28	1,50	1,00
07.11.2019 11:38	Interval	1,10	2,28	1,51	1,00
07.11.2019 11:38	Interval	1,10	2,28	1,52	1,00
07.11.2019 11:38	Interval	1,10	2,29	1,52	0,90
07.11.2019 11:38	Interval	1,10	2,29	1,52	1,00
07.11.2019 11:38	Interval	1,10	2,30	1,53	0,90
07.11.2019 11:38	Interval	1,10	2,31	1,53	0,90
07.11.2019 11:38	Interval	1,10	2,31	1,54	0,90
07.11.2019 11:38	Interval	1,10	2,31	1,54	0,80
07.11.2019 11:38	Interval	1,00	2,30	1,54	0,90
07.11.2019 11:38	Interval	1,00	2,32	1,53	1,00
07.11.2019 11:38	Interval	1,20	2,32	1,54	1,00
07.11.2019 11:38	Interval	1,10	2,32	1,54	1,00
07.11.2019 11:38	Interval	1,10	2,32	1,54	0,90
07.11.2019 11:38	Interval	1,20	2,33	1,54	0,90
07.11.2019 11:38	Interval	1,20	2,33	1,54	0,90
07.11.2019 11:38	Interval	1,20	2,34	1,54	0,90
07.11.2019 11:38	Interval	1,20	2,34	1,53	0,90
07.11.2019 11:38	Interval	1,20	2,35	1,54	0,90
07.11.2019 11:38	Interval	1,20	2,35	1,53	0,90
07.11.2019 11:38	Interval	1,20	2,35	1,54	0,90

07.11.2019 11:38	Interval	1,20	2,36	1,54	0,90
07.11.2019 11:38	Interval	1,10	2,37	1,54	1,00
07.11.2019 11:38	Interval	1,20	2,37	1,53	0,90
07.11.2019 11:38	Interval	1,20	2,37	1,54	0,90
07.11.2019 11:38	Interval	1,10	2,37	1,54	0,90
07.11.2019 11:38	Interval	1,10	2,38	1,54	0,90
07.11.2019 11:38	Interval	1,00	2,38	1,54	0,90
07.11.2019 11:38	Interval	1,00	2,38	1,54	0,90
07.11.2019 11:38	Interval	1,00	2,39	1,53	1,00
07.11.2019 11:38	Interval	0,90	2,39	1,54	1,00
07.11.2019 11:38	Interval	1,00	2,39	1,54	0,90
07.11.2019 11:38	Interval	0,90	2,39	1,54	0,90
07.11.2019 11:38	Interval	0,80	2,39	1,54	0,90
07.11.2019 11:38	Interval	0,80	2,40	1,54	0,90
07.11.2019 11:38	Interval	0,80	2,40	1,54	0,90
07.11.2019 11:38	Interval	0,80	2,40	1,54	0,90
07.11.2019 11:39	Interval	0,90	2,41	1,54	0,90
07.11.2019 11:39	Interval	0,70	2,41	1,54	0,90
07.11.2019 11:39	Interval	0,80	2,42	1,55	0,90
07.11.2019 11:39	Interval	0,80	2,42	1,56	0,90
07.11.2019 11:39	Interval	0,80	2,42	1,55	0,90

Appendix D: The difference in measured temperature of Thermocouple and PT1000 sensors.

	<b>Date/Time</b>	<b>tempAir ('C)</b>	<b>tempGround ('C)</b>
<b>Thermocouple</b>	18.11.2019 / 10.17.53	22.60	22.60
	18.11.2019 / 10.18.03	22.60	22.60
	18.11.2019 / 10.18.13	22.60	22.70
	18.11.2019 / 10.18.23	22.60	22.70
	18.11.2019 / 10.18.33	22.60	22.70
	18.11.2019 / 10.18.43	22.60	22.70
	18.11.2019 / 10.18.53	22.60	22.60
	18.11.2019 / 10.19.03	22.60	22.70
	18.11.2019 / 10.19.13	22.60	22.70
	18.11.2019 / 10.19.23	22.70	22.70
	18.11.2019 / 10.19.33	22.60	22.70
	18.11.2019 / 10.19.43	22.60	22.60
<b>PT1000</b>	18.11.2019 / 10.22.00	23.71	23.74
	18.11.2019 / 10.22.10	23.72	23.72
	18.11.2019 / 10.22.20	23.71	23.70
	18.11.2019 / 10.22.30	23.71	23.69
	18.11.2019 / 10.22.40	23.70	23.67
	18.11.2019 / 10.22.50	23.67	23.65
	18.11.2019 / 10.23.00	23.64	23.61
	18.11.2019 / 10.23.10	23.61	23.58
	18.11.2019 / 10.23.20	23.59	23.56
	18.11.2019 / 10.23.30	23.57	23.55
	18.11.2019 / 10.23.40	23.58	23.54
	18.11.2019 / 10.23.50	23.59	23.53